ADTEC

Semiannual Technical Report
Contract No. AF 30(602)-3495

HIGH POWER FERRITE PHASE SHIFTER

January 15, 1965

ADVANCED TECHNOLOGY CORPORATION
1830 YORK ROAD TIMONIUM, MARYLAND

DISCLAIMER NOTICE

THIS DOCUMENT IS THE BEST QUALITY AVAILABLE.

COPY FURNISHED CONTAINED A SIGNIFICANT NUMBER OF PAGES WHICH DO NOT REPRODUCE LEGIBLY.

HIGH POWER FERRITE PHASE SHIFTER

Prepared for

Rome Air Development Center
Air Force Systems Command
United States Air Force
Griffiss Air Force Base
New York

Semiannual Technical Report
Contract No. AF 30(602)-3495
ARPA Order No. 550
Program Code No. 4730

January 15, 1965

ADVANCED TECHNOLOGY CORPORATION
1830 York Road
Timonium, Maryland

Project Engineer: Frederick L. Wentworth

SYNOPSIS

Theoretical and experimental investigations of the microwave properties of ferrites at magnetic fields above ferromagnetic resonance are described. The program goal is the development of high power reciprocal phase shifters for X-band and C-band operation. The principal experimental objective is to demonstrate that ferromagnetic losses do not increase with the application of high RF power as typically observed for operations at magnetic fields below resonance. Insertion losses are given as a function of magnetic field strength for samples of nickel-zinc ferrite, manganese-magnesium ferrite and yttrium-iron garnet in a longitudinally magnetized rod configuration. A second absorption peak on the high side of resonance was observed and is identified as a body resonance. The data demonstrates that, at a fixed frequency, the second peak moves toward the ferromagnetic resonance peak as the cross sectional dimensions are reduced.

Insertion loss and phase shift characteristics for oriented uniaxial ferrites are given. The material investigated was $Ni_{.8}Zn_{.2}Co_{.02}W$, a ferrite having a hexagonal crystal structure. It was established that uniaxial ferrites would not be suitable for the subject application because of poor figures of merit. Theoretical computations showed that the governing material characteristic that leads to a poor figure of merit is a large linewidth. The W-type, polycrystalline ferrite typically has a linewidth of 2000 oersteds, which is an order of magnitude larger than that of nickel-zinc ferrite (a cubic crystal structure).

A derivation of the complex susceptibility for ferromagnetic materials and a set of generalized curves for rod geometries with longitudinal magnetic fields are given in the Appendix.

TABLE OF CONTENTS

LIST OF ILLUSTRATIONS

LIST OF ILLUSTRATIONS (Continued)

I. INTRODUCTION

This program is a design study to develop reciprocal ferrite phase shifters for both C- and X-bands with the capability of handling a peak power of 100 kilowatts and an average power of 1 kilowatt at less than a 1 db loss. A total phase shift of 360° in 10 microseconds with an expenditure of less than 150 micro joules for switching is desirable. In order to achieve these goals three major problems must be overcome:

(1) Elimination of nonlinear losses due to high peak power

(2) Control of temperature at high average power

(3) Design of biasing fields for microsecond switching.

The contractor's proposed approach to these problems is summarized as follows:

(1) The increased RF losses in ferrites as a function of increased power are observed by the appearance of a subsidiary resonance peak below the main resonance and by the broadening of the main resonance absorption line. The subsidiary resonance may be avoided by operating the ferrite at magnetic fields above the main resonance. By operating still farther above resonance, one can decrease the additional losses incurred by broadening of the main resonance line.

(2) The temperature control at high average power operation will be obtained by the circulation of a low loss liquid coolant (Freon 113, for example) through the phase shifter and an external heat exchanger. This technique has been used successfully by the contractor for temperature control of a UHF Y-circulator operating at 2 kilowatts average power.

(3) In the more conventional phase shifters, which use a ferrite in metallic waveguide and axial magnetic fields, the switching speed is retarded by the shorted turn currents in the waveguide walls. The contractor has proposed to eliminate the shorted turn effect by substituting a dielectric rod waveguide , consisting of the ferrite

itself, for that part of the metallic waveguide within the solenoid. Because of the large dielectric constant of the ferrite (10 to 16), a dielectric rod transmission line which confines more than 90% of the transmitted energy in the rod can be achieved with a diameter smaller than the narrow dimension of a standard waveguide. It has been recognized that a fundamental objection to the HE_{11} mode in dielectric rod transmission is that rotation of the plane of polarization is permitted. This is in direct conflict with conventional applications which use fixed polarization, rectangular waveguide. In order to eliminate rotation, the proposed design employs an image plane dielectric transmission line with a half round dielectric rod on a conducting ground plane rather than the full round dielectric rod.

The contractor is not limiting his attention to this configuration, however, since other solutions to the shorted turn effect have been found to be satisfactory. The primary goal is to demonstrate the absence of the nonlinear losses at high peak power operation.

II. FERRITE MATERIALS

Ferrite characteristics involve a number of parameters which are interrelated by the material chemistry, fabrication techniques, and component configuration. The equations which follow describe the relationship of the principal characteristics in the phase shifter application. It is important to recognize the several possibilities for trade-off of values among the various parameters.

The frequency, f_r, at ferromagnetic resonance is given by

$$f_r = \gamma H_{eff}, \tag{1}$$

where

f_r = ferromagnetic resonance frequency in megacycles

γ = gyromagnetic ratio, approximately 2.8 megacycles per oersted

H_{eff} = effective internal magnetic field in oersteds,

where

$$H_{eff} = H_o + 2\pi M_s + H_a, \tag{2}$$

where

H_o = externally applied magnetic field

$2\pi M_s$ = demagnetizing field of an axially magnetized rod, and

H_a = anisotropy field which will be parallel to H_o.

On combining these equations, one may arrive at an expression for the externally applied field at resonance

$$H_o = \frac{f_r}{\gamma} - 2\pi M_s - H_a. \tag{3}$$

The proposed high power phase shifter requires a still greater magnetic field to reach the low loss region above resonance. The magnitude of this additional field cannot be specified since the absolute loss of the phase shifter depends upon the total length of ferrite rod required for the 360^o phase shift. This, in turn, is dependent upon the activity of the ferrite in the region of the magnetic bias field. A figure of merit,

giving phase shift per db loss, is often used to appraise the quality of a phase shifter. The magnetic bias field which gives the best figure of merit is most easily determined experimentally. The additional magnetic field above resonance required to reach this point, however, can be estimated from the line width of the ferrite. A comparison of the material characteristics for a number of Trans-Tech's garnets indicates that the line width 15 db down from the peak ($0.0316\ \chi''_{max}$) is approximately 4 times that at the -3db point ($0.5\ \chi''_{max}$). On adding the additional field of $4(\frac{\Delta H}{2})$ to Equation 3, one gets

$$H_o = \frac{f}{\gamma} - 2\pi M_s - H_a + 2\Delta H \qquad (4)$$

as an estimate of the required external field for operation at the frequency f. Since H_o is to be supplied by a permanent magnet, the upper limit is set at 1200 oersteds, which can be realized by using an Alnico-8 tubular magnet 6 cm long, 3.25 cm I.D. and 7 cm O.D. With a magnet 12 cm long, the upper limit is set at 760 oersteds.*

The specifications for an acceptable ferrite material are, therefore, given by Equation 4 where the frequencies of interest are 9400 Mc and 5500 Mc and $H_o < 1200$ oe and $H_o < 760$ oe, respectively. In general, it is desired to minimize H_o; thus, γ, M_s and H_a should be large and ΔH should be small. Additional specifications for the material are:

Dielectric loss tangent	< 0.001
Dielectric constant	> 10
Curie temperature	$> 100^{\circ}C$

Furthermore, all of the characteristics should have minimum temperature sensitivity. In ferrites having a cubic crystal structure the anisotropy field, H_a, is typically small, unoriented and nominally taken to be zero. In ferrites having a hexagonal crystal structure[1, 2] the anisotropy fields are large and may be oriented during the fabrication in a desired direction within the sample. The magnitude of the anisotropy field has been

---

*Private communication with Irene Wagner, Crucible Steel, Magnet Division, Harrison, N.J.

the subject of a number of investigations,[3, 4] and as a result it is readily predictable on the basis of the material chemistry and fabrication techniques. The utilization of hexagonal ferrites with a uniaxial (along the C axis) anisotropy field oriented in the direction of the applied field is especially attractive for X-band operation above ferromagnetic resonance, where the requirement for high internal magnetic fields precludes the use of isotropic ferrites.

An important consideration in high power applications of ferrites is their temperature sensitivity. Ideally, the operating frequency indicated by a rearrangement of Equation 3,

$$f = \gamma(H_o + H_a + 2\pi M_s - 2\Delta H), \tag{5}$$

should not change with temperature variation. In Equation 5, which is for an axially-magnetized rod configuration, it is seen that the term for the demagnetizing field, $2\pi M_s$, is positive. Since H_a has a positive temperature coefficient (depending upon doping*) and M_s has a negative temperature coefficient, Equation 5 allows us to predict that the temperature sensitivity will be reduced. The anticipation of some temperature compensation is pointed out here because earlier investigators of oriented ferrites have revealed unfavorable temperature sensitivities. In the application of the earlier work, transverse magnetic fields on slab geometries were used. The demagnetization term, in that case, is negative; thus, the temperature sensitivities of M_s and H_a are additive.

---

*Referenced example is Nickel Cobalt W ferrite, see Ref. 3.

III. EXPERIMENTAL (FERRITES WITH CUBIC CRYSTAL STRUCTURES)

The proposed design for a reciprocal phase shifter to operate at X-band was fabricated using a nickel-zinc ferrite, Trans-Tech TT2-111. The material was chosen for its high saturation moment and narrow linewidth as per Equation 4. The pertinent characteristics of TT2-111 are as follows:

Saturation Moment, $4\pi M_s$	= 5000 gauss
Linewidth, ΔH	= 135 oersteds
Dielectric Constant, ϵ_r	= 12.5
Dielectric loss tangent, tan δ	= 0.001
Curie Temperature, T_c	= 375°C
Effective g	= 2.08.

A cut-away drawing of the first model is shown in Figure 1. The ferrite was ground to 0.395-inch diameter and to a length of 4 inches. Conical transition sections of Stycast* -15 (ϵ_r = 15) were attached to both ends. The whole assembly was placed in a solenoid which could provide up to 1400 oersteds.

Measurements on this first configuration gave an insertion loss considerably higher than expected (> 10 db) over the tested range of magnetic field from 0 to 1400 oersteds and frequency from 8 to 12 Gc. The input VSWR was, at some points, as high as 4:1. The high VSWR was attributed to poor surface wave launching onto the ferrite rod. In order to test the launching question, a Stycast-15 rod was made to the same dimensions as the ferrite sample. By adjusting the position of the taper sections in the rectangular waveguide, a VSWR of 1.1 at 9375 Mc was realized. The VSWR over the frequency band from 8 to 11 Gc subsequently was found to be less than 1.4. The insertion loss at 9375 Mc was 0.7 db and over the frequency band it was less than 2 db. The Stycast-15 test showed that a low loss surface wave was

---

*Registered Trade-Mark of Emerson and Cumings, Inc.

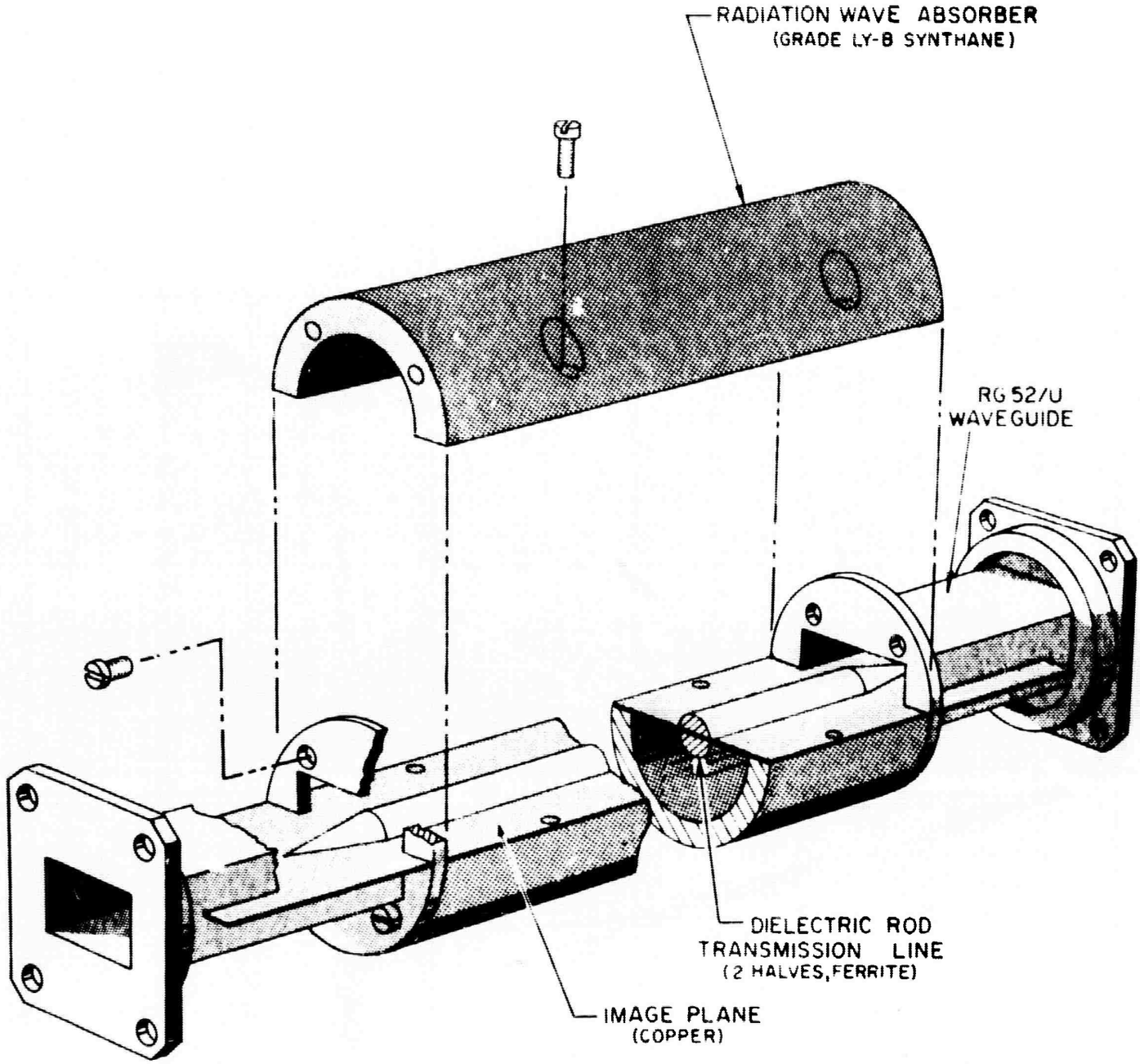

FIG. 1 -MODEL, TWIN IMAGE LINE FERRITE PHASE SHIFTER

achievable with the proposed twin image line configuration; it further indicated the most favorable position of the taper with respect to the open waveguide launchers. The ferrite rod was tested a second time for launching efficiency after making a minor modification to incorporate the data gained from the Stycast-15 test. The input VSWR was satisfactory, but the insertion loss was still high. Another possible explanation for the high insertion loss was a suspected mismatch at the interface between the Stycast-15 transitions and the ferrite; consequently, a new ferrite rod having conical tapers was ground from one piece of TT2-111. A simplification in the test setup was also made by taking the loss measurements with a whole rod in a section of standard waveguide rather than in the configuration shown in Figure 1. The resulting losses at 9 Gc, 10 Gc, and 11 Gc as a function of magnetic field for the one-piece specimen are shown in Figure 2. Also shown is the insertion loss at 11 Gc for the ferrite specimen with Stycast transitions. Note that the minimum loss in the one-piece ferrite is considerably less. It appears that the Stycast-ferrite interfaces introduce additional loss; however, since ferrite characteristics vary between specimens, some of this difference may be attributed to a poorer piece of ferrite. This data should be compared to that concerning the insertion loss for a Stycast-15 rod, which is only 0.3 db over the frequency band. The dissipation factor of Stycast HiK material is approximately 0.002.

Figure 2 further shows that on the high side of resonance at 9 Gc, the insertion loss remains high. These results, supported by the earlier measurements, indicate that the primary source of high insertion loss is in the TT2-111 ferrite. It should be pointed out that the characteristics of TT2-111 on the high side of resonance were not known; but, assuming a well-behaved resonance characteristic, it was estimated (Equation 4) that a low loss region would be found at 9.4 Gc for fields above 1120 oersteds. A re-examination of the resonance characteristic for TT2-111 was requested from Trans-Tech. The results of this

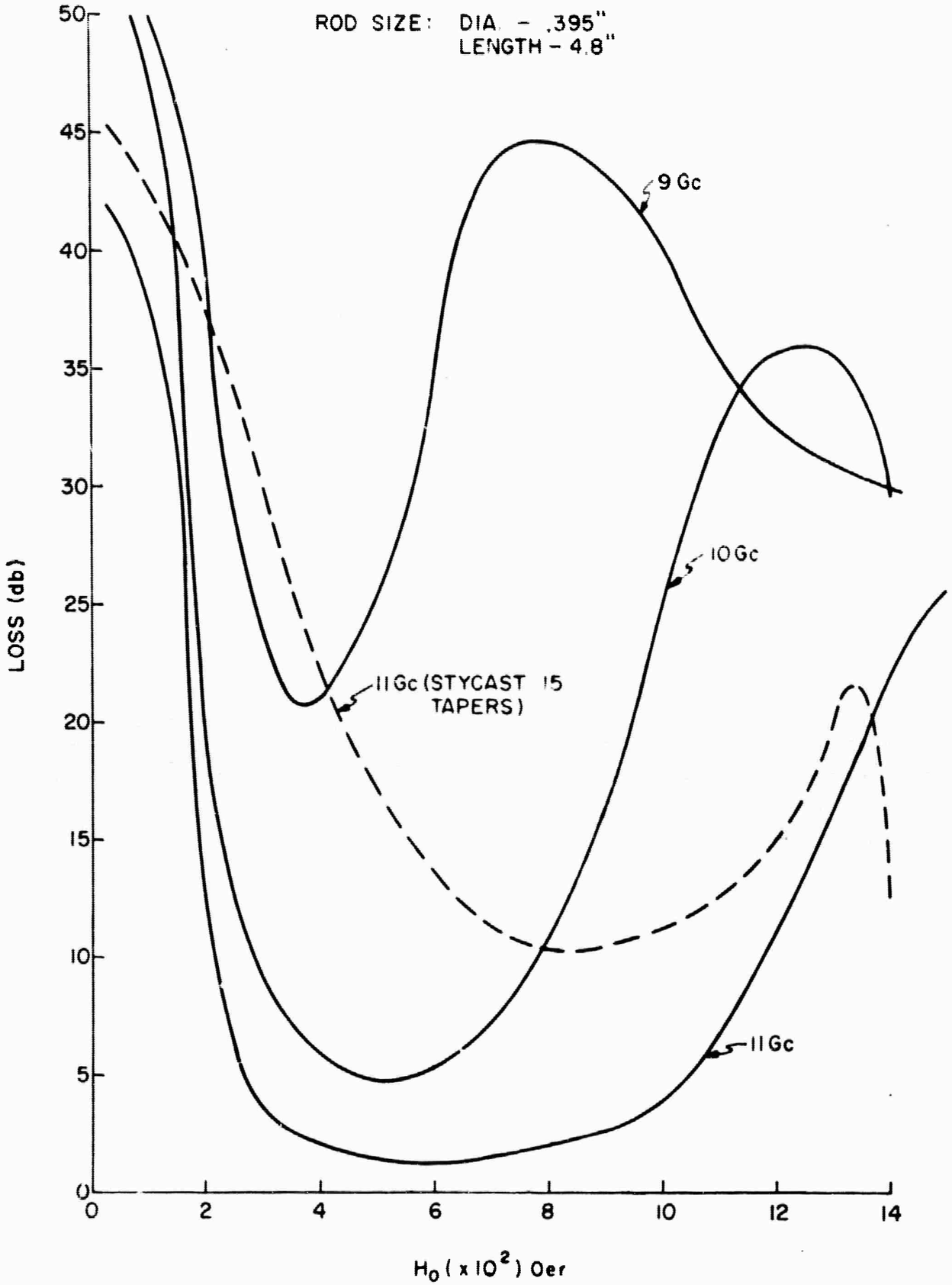

FIG. 2 - LOSS CHARACTERISTICS OF TT2-111 FERRITE ROD IN RG 52/u WAVEGUIDE.

measurement, which used a crossed waveguide coupler method,[5] are given in Figure 3. Stinson has shown that the linewidth is given by the magnetic field between the -3 db points on such a curve. Note that a second absorption peak appears on the high side of resonance and, as a consequence, the magnetic field at the -15 db point is 830 oersteds above resonance rather than 270 oersteds as estimated on the basis of $2\Delta H$. With this correction, Equation 4 enables one to predict that the field required to reach the low loss region is 1690 oersteds. Therefore, it was concluded that TT2-111 would be unsuitable for X-band operation.

It is speculated that the double peak resonance characteristic of TT2-111 is caused by the unoriented anisotropy fields. In the cubic ferrites these fields are on the order of 100-200 oersteds. The relationship between the anisotropy field and the two resonance peaks has been indicated by Viehmen[6] in his work with hexagonal ferrites. If it is assumed that the magnetic fields at the first and second peaks indicate resonances for the applied field parallel (H_E) and perpendicular (H_H) respectively to the anisotropy fields, one may use the following relationship given by Rodrique[3] to compute the anisotropy field:

$$H_a = -\left(\frac{2H_E + H_H}{2}\right) + \sqrt{\left(\frac{2H_E + H_H}{2}\right) + H_H^2 - H_E^2} \quad . \tag{6}$$

For TT2-111 $H_a = 208$ oersteds,

where $H_E = 3120$ oersteds,

and $H_H = 3435$ oersteds.

Two schemes for eliminating the second absorption peak (provided it is truly caused by the anisotropy fields in the material) are immediately obvious. The first is to orient the anisotropy field. If the direction is chosen parallel to the applied field, the anisotropy field could be used to an advantage in the phase shifter application. It is understood* that orienting the anisotropy fields in cubic ferrites has been considered

---

*Private communication with L.R. Hodges, Jr., Sperry Microwave Electronics Company, Clearwater, Florida.

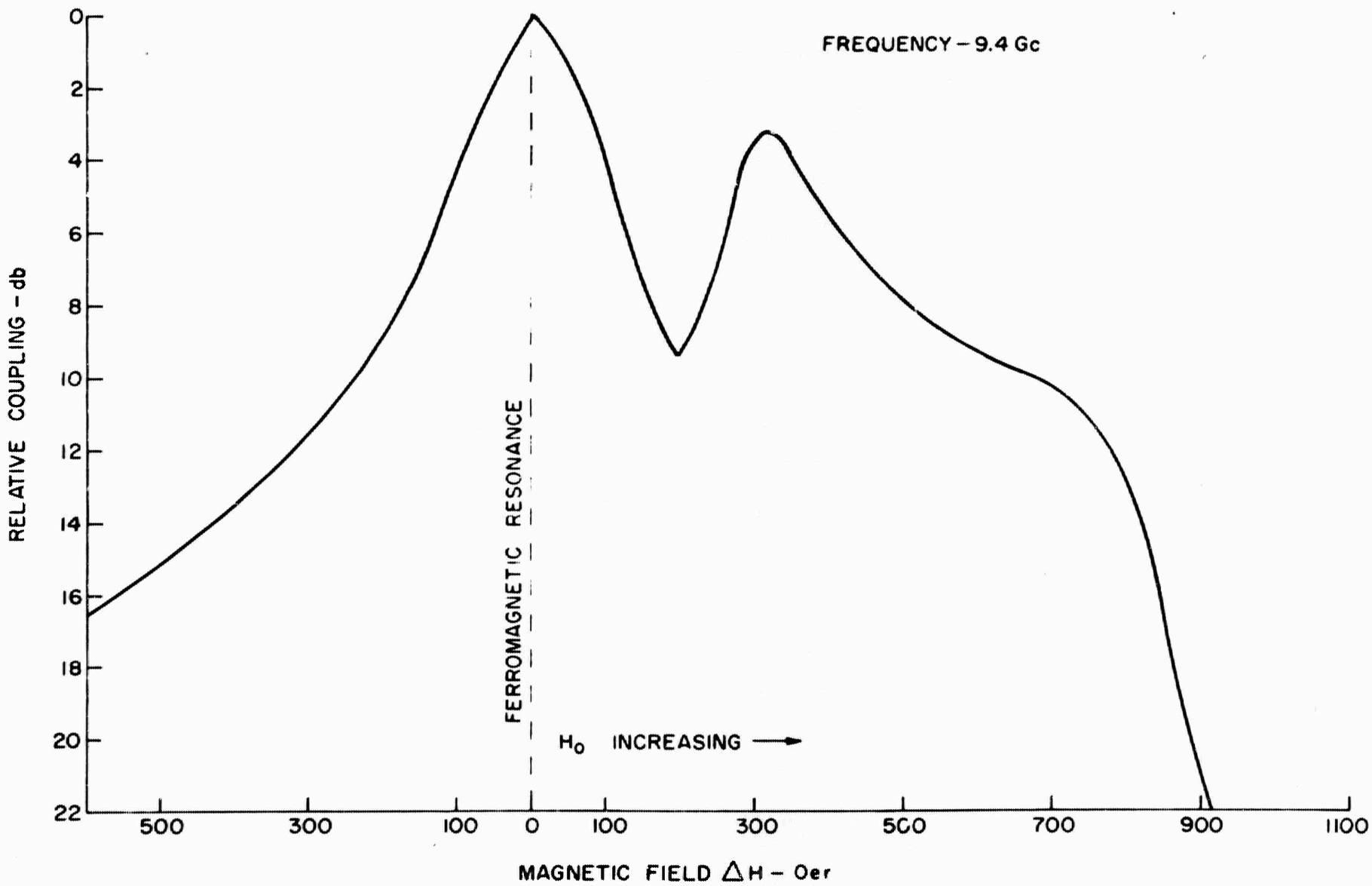

FIG. 3 – RESONANCE CURVE FOR TT2-III (COURTESY TRANS-TECH)

but due to their small magnitude the desired results have not been accomplished.

The second method would be to minimize the anisotropy field. Pippin and Hogan[7] have shown that the anisotropy fields can be reduced to zero by making small additions of cobalt to nickel ferrites. A sample of $Ni_{.8}Z_{.2}Co_{.025}$ ferrite was purchased from Sperry Microwave Electronics Company. The sample is designated No. 98-B and has the following characteristics:

$4\pi M_s = 4490$

$\Delta H = 200$ oersteds

$\tan \delta = 0.002$

$\epsilon_r = 12.5 - 15$ (not given)

$T_c =$ (not given)

$g =$ (not given).

The material has not been fully evaluated, but preliminary measurements show a disappointingly high loss.

Because of the unsuccessful attempts to find a low loss region above resonance at X-band with ferrites having a cubic crystal structure, the investigation was moved to C-band to permit the survey of cubic ferrite materials having lower values of saturation moment.

A problem has been encountered in the measurements at C-band for which a solution is presently being sought. In the insertion loss measurements a second absorption peak above ferromagnetic resonance has been observed and is believed to be a body resonance which exists when the ferrite is large enough to sustain a cavity-type mode The identification of the second peak was made after observing that as the thickness of the ferrite was reduced, the body resonance peak moved toward the stationary ferromagnetic peak. At a constant frequency, a larger value of effective permeability is required to explain the continued presence of a resonant peak even after the ferrite dimensions have been reduced. This is consistent with the fact that on the high side

of resonance, permeability increases as the magnetic field approaches the ferromagnetic resonance value.

The material survey at C-band was begun with TTG-113, an yttrium-iron garnet having the following characteristics:

$$4\pi M_s = 1725 \text{ gauss}$$
$$\Delta H = 55 \text{ oersteds}$$
$$\epsilon_r = 16$$
$$\tan \delta = 0.00025$$
$$T_c = 280$$
$$g = 2.01$$

Due to the low saturation moment, ferromagnetic resonance was observed at a frequency of 5.5 Gc with a magnetic field strength of 1300 oersteds. Since the present test setup cannot provide field strengths of more than 1800 oersteds, the study of ferromagnetic behavior above resonance was extended down to 4.0 Gc, where resonance occurred at 750 oersteds. The loss characteristics as a function of thickness were measured on a slab 0.385 inch wide and 3.437 inches long. Figures 4, 5, and 6 show this data for 4 Gc, 4.5 Gc, and 5 Gc, respectively. It will be noted that the first resonance peak is stationary, while the second peak moves toward the first as the thickness is reduced. At 5 Gc, with the thicker samples, several peaks were observed (not shown in Figure 5) indicating higher order body modes.

The desirability of obtaining a ferromagnetic material with a narrow linewidth for above-resonance operation was demonstrated in these measurements on garnet. If the body resonance is disregarded ferromagnetic losses appear to decrease rapidly with field strength on the high side of resonance and values less than 0.5 db were measured for the three-inch sample. The usefulness of garnet proved to be limited to frequencies below 5 Gc. Therefore, it was apparent that materials having larger saturation moments would be required for operation in the desired frequency band (5.5 to 7.5 Gc).

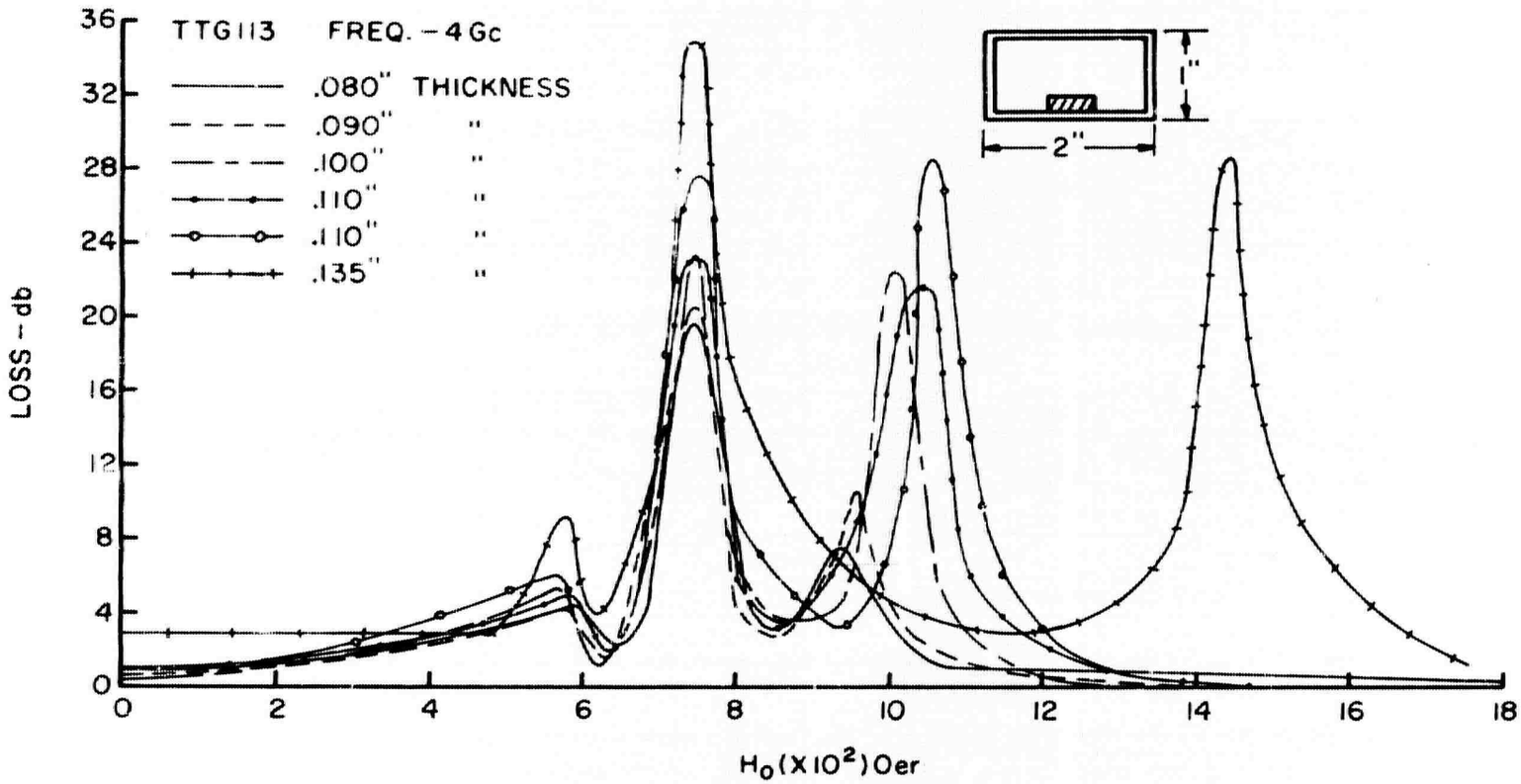

FIG. 4 – INSERTION LOSS CHARACTERISTICS OF YITTRIUM IRON GARNET, AS A FUNCTION OF THICKNESS, AT 4 Gc.

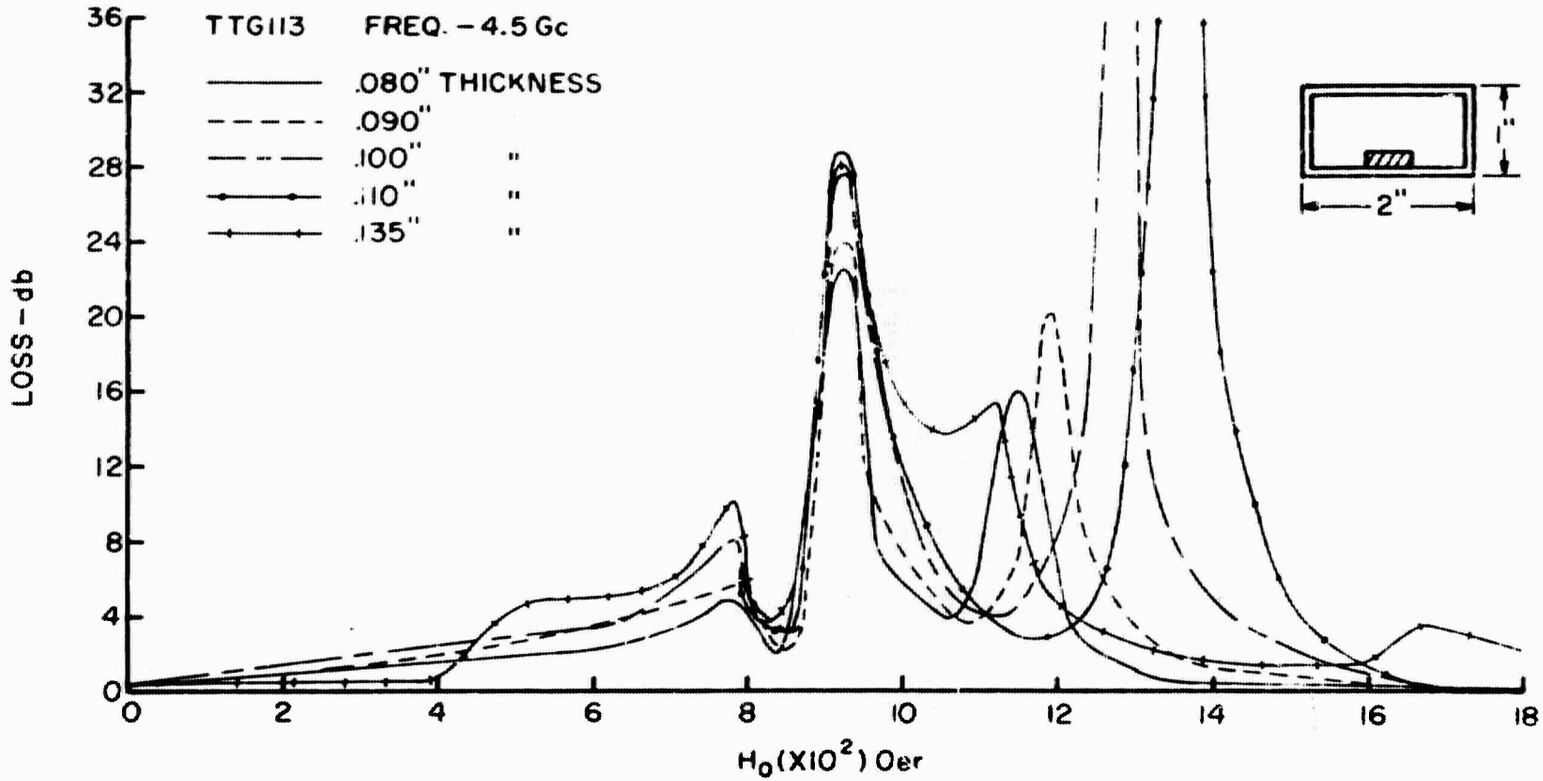

FIG. 5 - INSERTION LOSS CHARACTERISTICS OF YITTRIUM IRON GARNET, AS A FUNCTION OF THICKNESS, AT 4.5Gc.

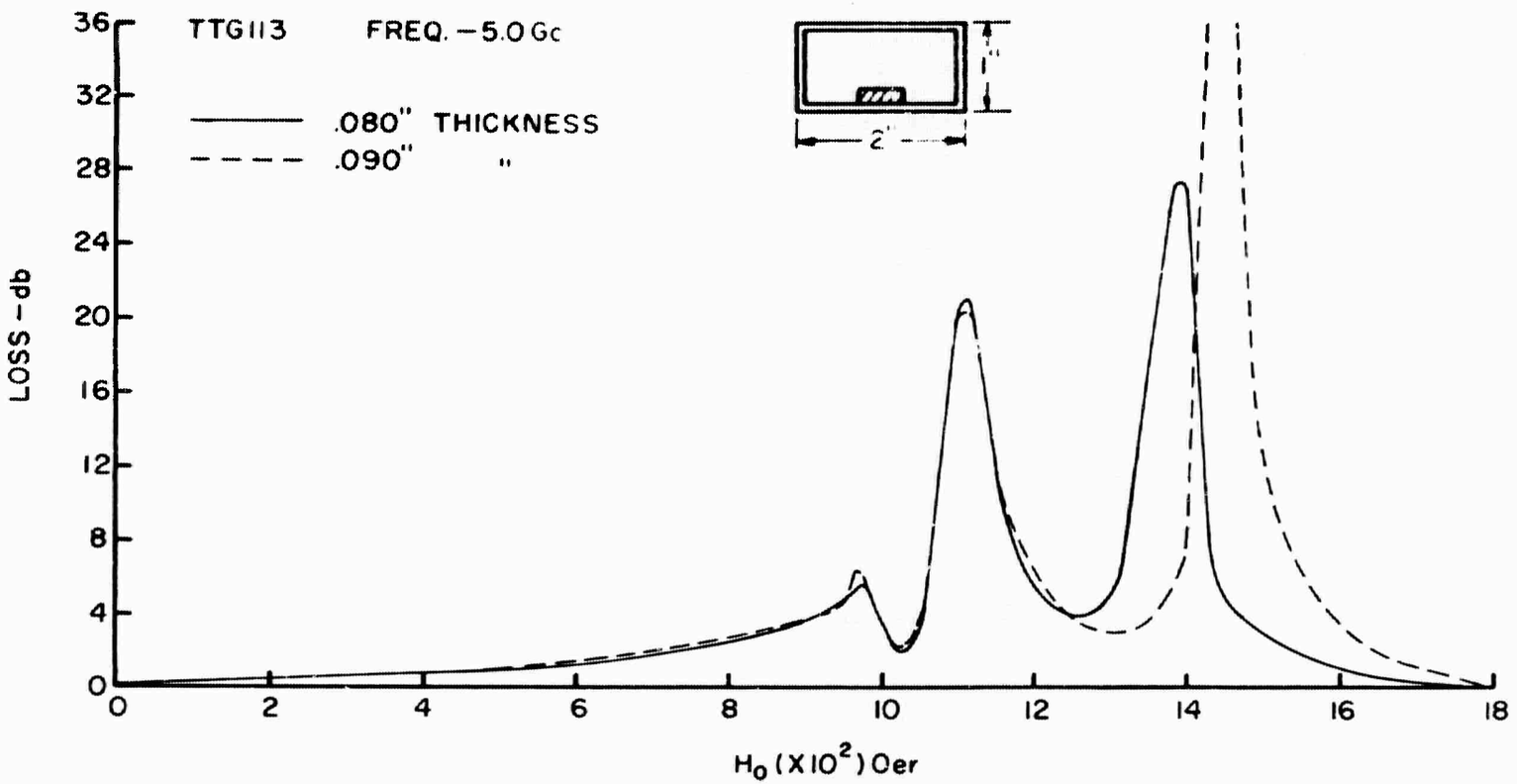

FIG. 6 - INSERTION LOSS CHARACTERISTICS OF YITTRIUM IRON GARNET, AS A FUNCTION OF THICKNESS, AT 5.0Gc.

A magnesium-manganese ferrite, Trans-Tech TT1-390, with the following characteristics was tested:

$4\pi M_s = 2150$ gauss

$\Delta H = 540$ oersteds

$\epsilon_r = 13$

$\tan \delta = 0.00025$

$T_c = 320^{\circ}C$

$g = 2.1.$

Ferromagnetic resonance occured at a frequency of 5.5 Gc and a magnetic field of 1000 oersteds. The detrimental effect of a large linewidth is demonstrated in Figure 7 by the existence of sustained high loss above resonance (16 db at 1800 oersteds in a four-inch sample). No further tests were made with this ferrite.

The evaluations of TTG-113 and TT1-390 were performed on samples with small rectangular cross sections. Since TT2-111 has both a high saturation moment ($4\pi M_s = 5000$ gauss) and a relatively narrow linewidth ($\Delta H = 135$ oersteds), it was decided to re-evaluate this material in the thin slab configuration. A rod of TT2-111, 0.4 inch in diameter, was tested and the losses were prohibitive. In a thin slab geometry, the results are more encouraging. Figures 8, 9, and 10 show the insertion loss characteristics as a function of thickness for a slab 0.4 inch wide and 4.375 inches long. Ferromagnetic resonance was observed for the following conditions of frequency and magnetic field:

5.5 Gc and 410 oersteds

6.5 Gc and 730 oersteds

7.5 Gc and 1100 oersteds.

In Figure 8, it is seen that the insertion loss for the 0.060 inch thick ferrite decreases rapidly on the high side of resonance and reaches 1.2 db at 1800 oersteds. It is believed that upon the elimination of the second peak, such a ferromagnetic resonance characteristic would

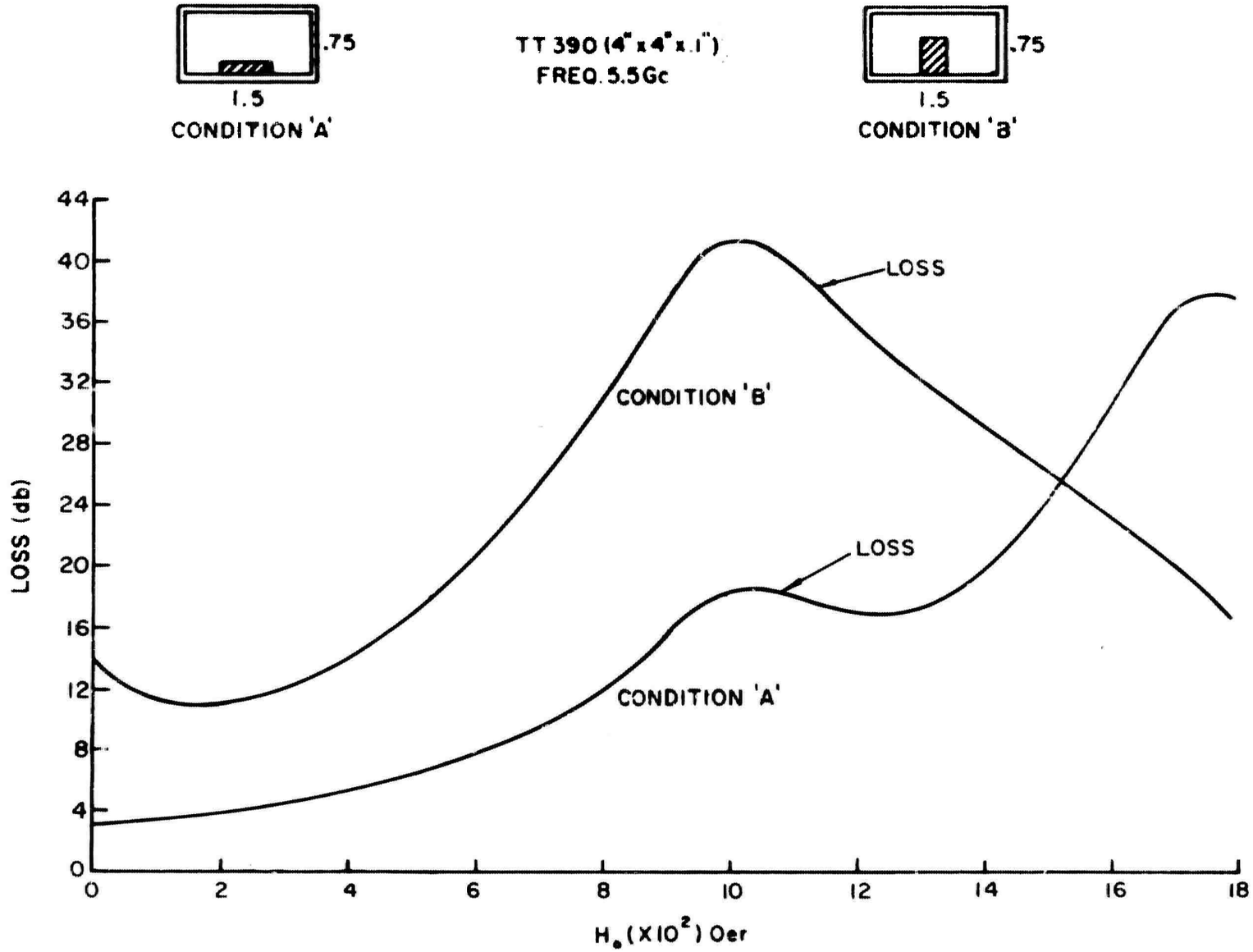

FIG. 7 - INSERTION LOSS FOR A MAGNESIUM-MANGANESE FERRITE, TRANS TECH TTI-390 FOR TWO CONFIGURATIONS AT 5.5 Gc

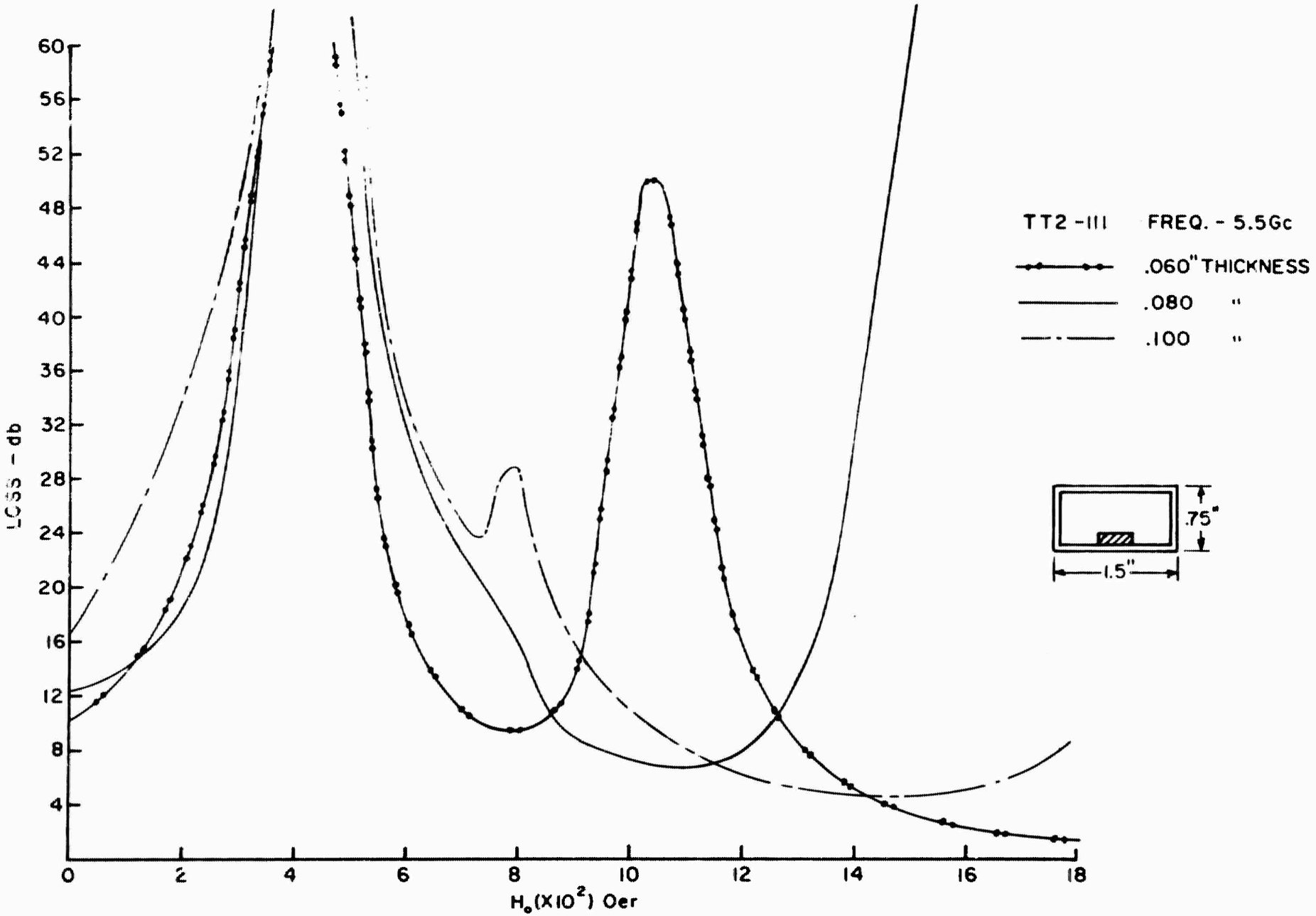

FIG.8 –INSERTION LOSS CHARACTERISTS OF A NICKEL ZINC FERRITE, AS A FUNCTION OF THICKNESS, AT 5.5 Gc.

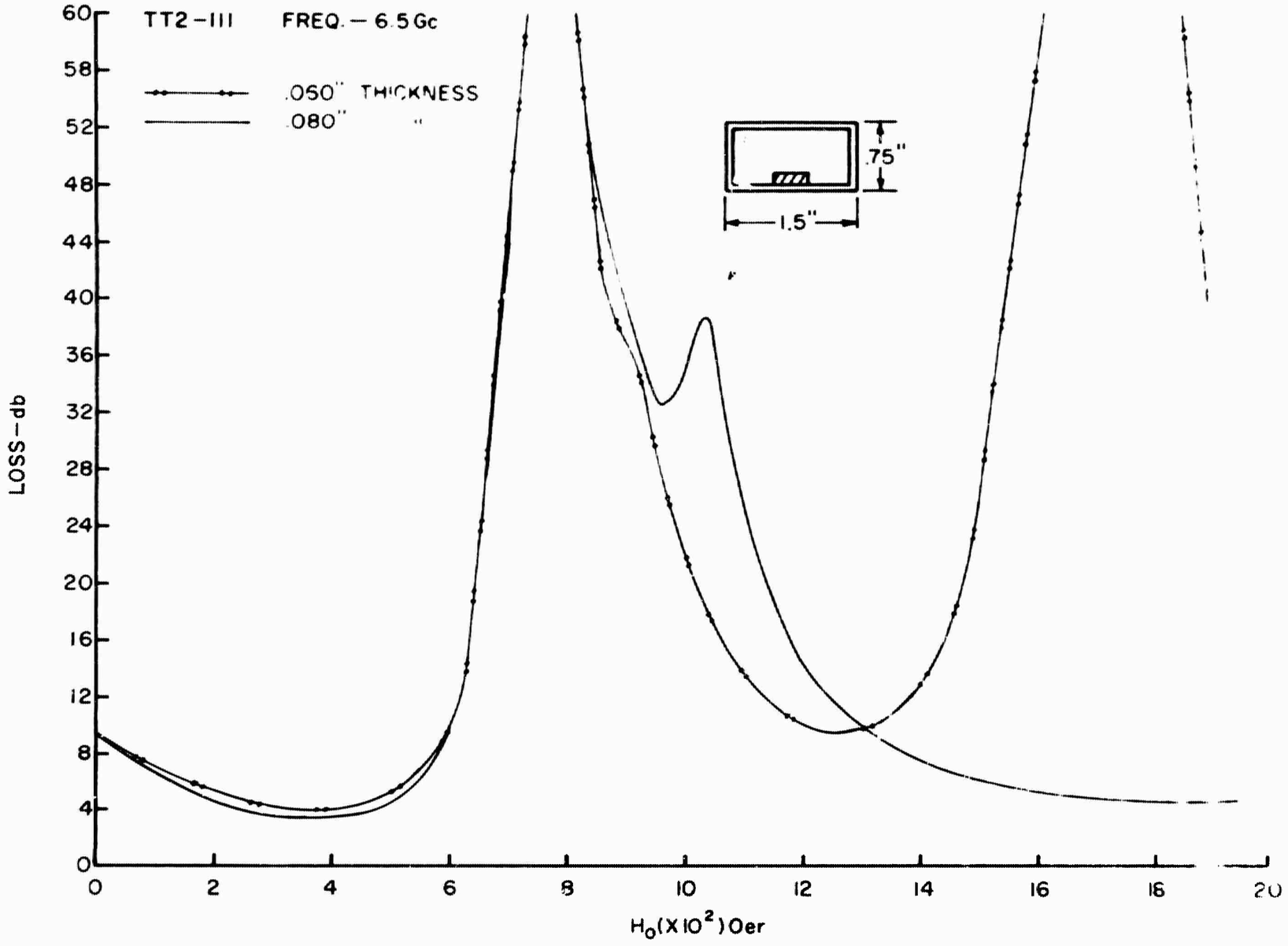

FIG. 9 - INSERTION LOSS CHARACTERISTS OF A NICKEL ZINC FERRITE, AS A FUNCTION OF THICKNESS, AT 6.5 Gc.

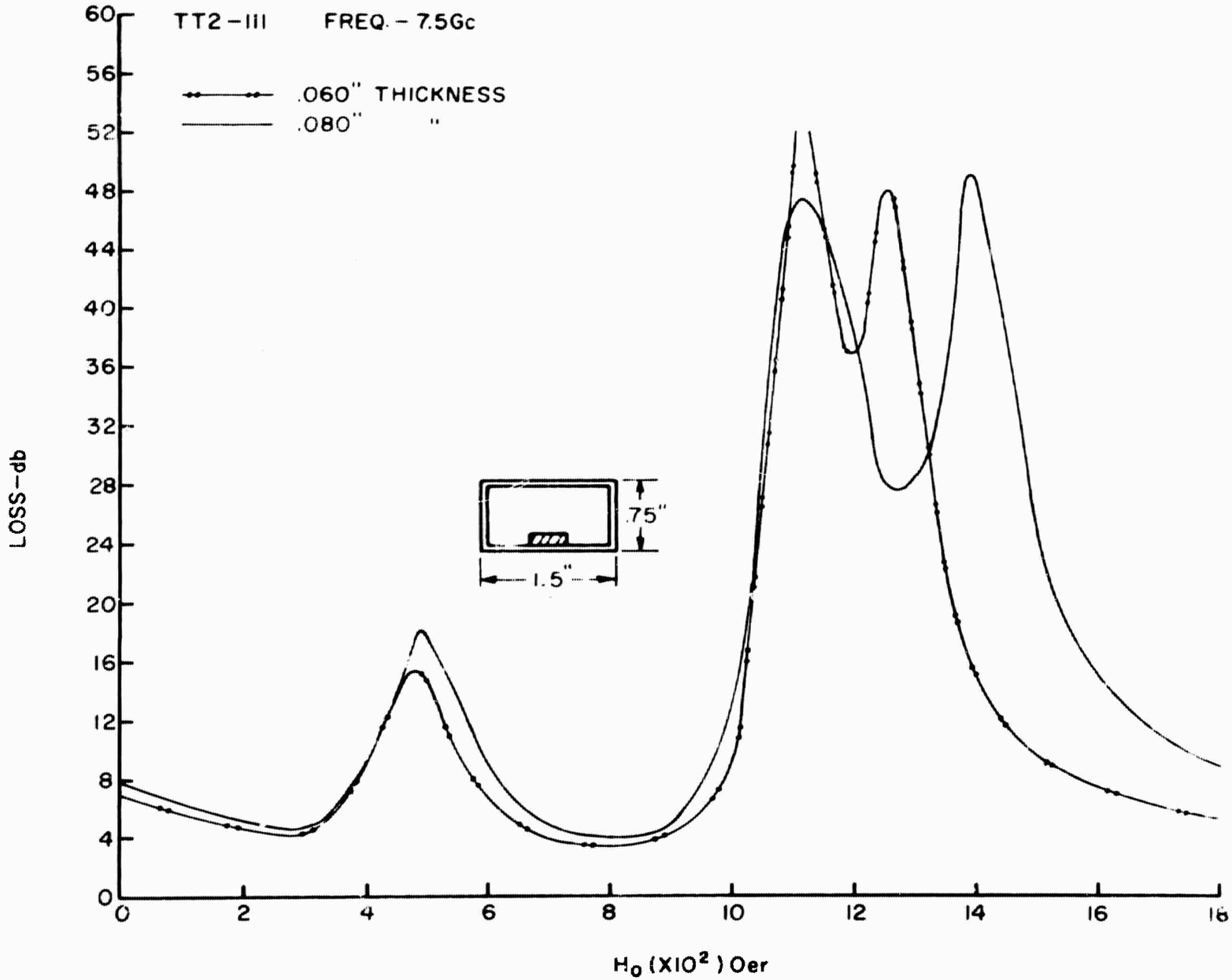

FIG.10-INSERTION LOSS CHARACTERISTS OF A NICKEL ZINC FERRITE, AS A FUNCTION OF THICKNESS, AT 7.5 Gc.

be acceptable. It remains to be seen whether satisfactory phase shift will also be achieved.

The ferrite slab-in-waveguide configuration shown in Figure 10 typically gives poor phase shift characteristics. However, if the ferrite is positioned as shown in Figure 11, considerably more activity is observed. Unfortunately, the loss associated with the activity in Figure 11 is quite large. This loss is still attributed to dimensional resonance.

The obvious solution to dimensional resonance difficulties is to reduce the ferrite size so that the relevant dimensions are less than a half wavelength inside the ferrite. The wavelength inside the ferrite is the free-space wavelength reduced by $(\mu_r \epsilon_r)^{-\frac{1}{2}}$, where typically the dielectric constant, $\epsilon_r = 12.5$, and the effective permeability is a function of the magnetic field. The theoretical values of the complex permeability for TT2-111 have been computed and are given in Figure 12. If a representative value of the dispersive component, $\mu' = 8$, is chosen; then it is seen that ferrite dimensions based on a 10:1 reduction from free-space wavelength are needed to suppress body resonance. Experimental evidence has shown that reduced size results in reduced activity, and this is to be expected since waveguide loading by the ferrite is also reduced. It is speculated that the ferrite activity may be recovered by reducing the dimensions of the associated waveguide. The proportionally larger ferrite then would have a greater effect in waveguide loading. In the work on ferrites with cubic structures during the third quarter these ideas will be explored.

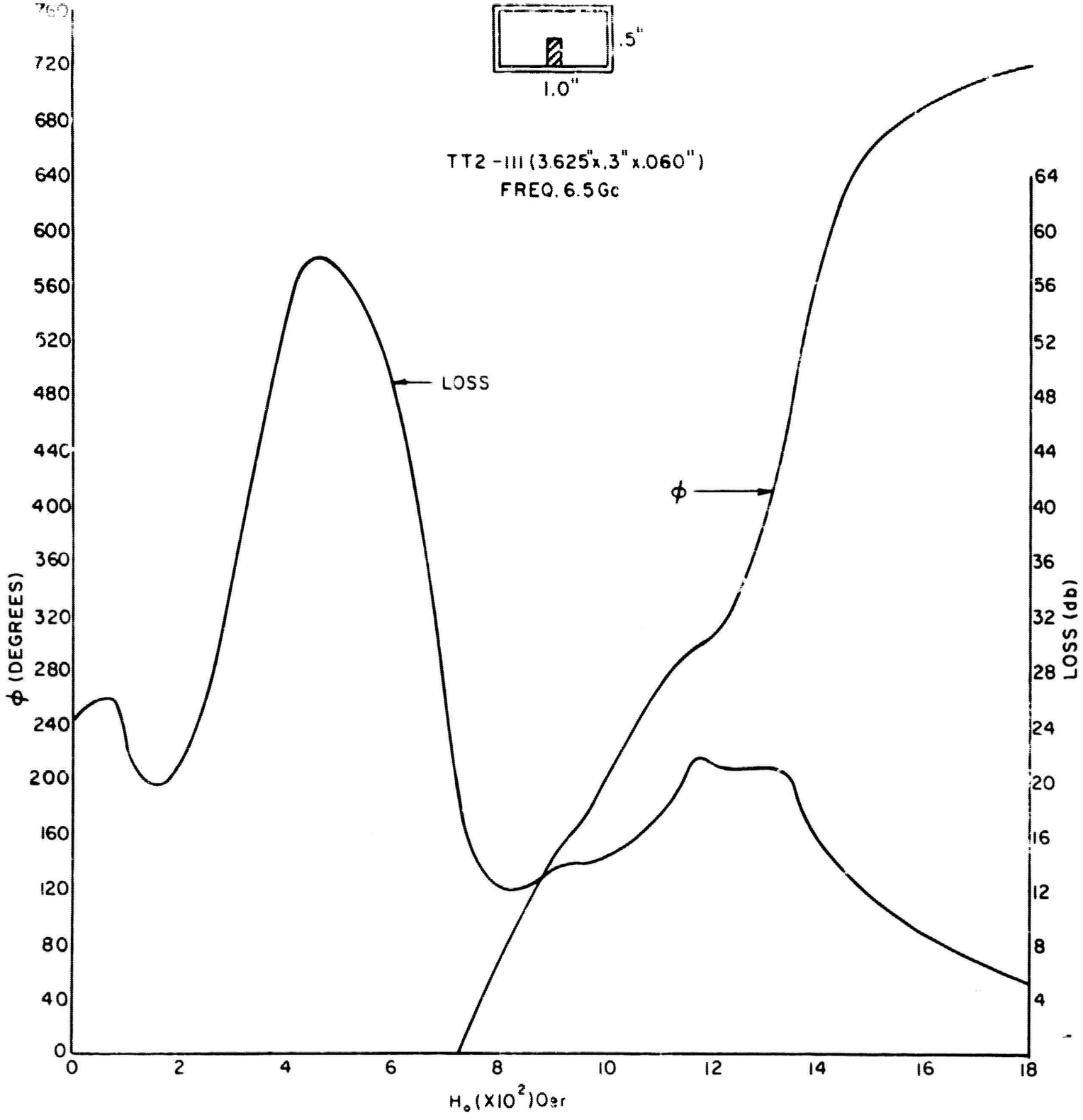

FIG. 11 - INSERTION LOSS AND PHASE SHIFT CHARACTERISTICS FOR TT2-III AT 6.5 Gc

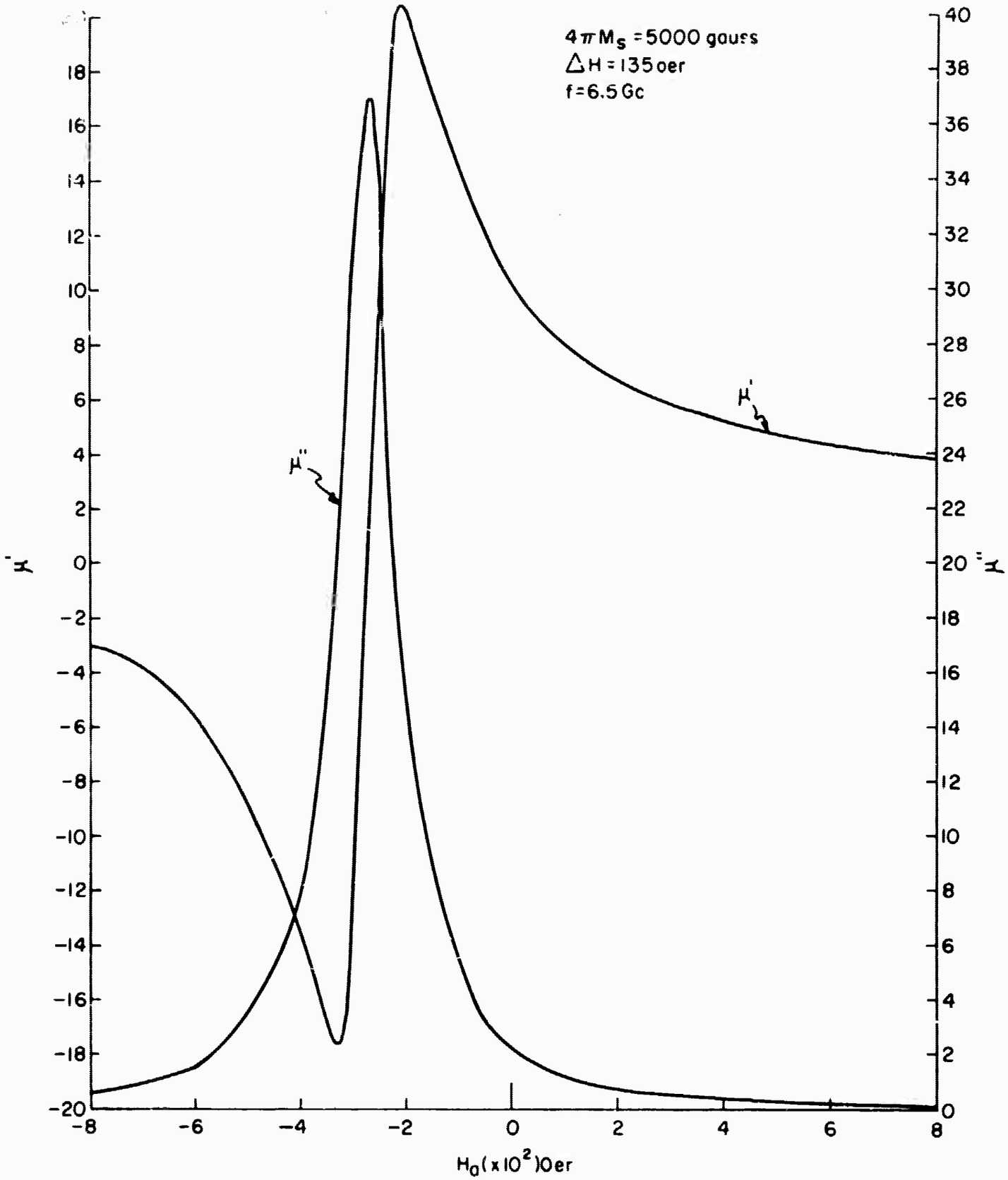

FIG. 12 - THEORETICAL COMPONENTS OF THE COMPLEX PERMEABILITY FOR TT2-111 AT 6.5 Gc.

IV. EXPERIMENTAL (FERRITES WITH HEXAGONAL CRYSTAL STRUCTURES)

Tentatively, it has been concluded that ferrites having cubic crystal structures would not be suitable for X-band operation because the required magnetic field is too high. (In the event that materials having higher saturation moments, $4\pi M_s > 6000$, become available, this conclusion should be reconsidered.)

An immediate solution to the high field requirement is available with the use of ferrites having hexagonal crystal structures. These materials have high anisotropy fields, and techniques for orienting these fields during fabrication have been established. In the large class of oriented ferrites having hexagonal crystal structures, there are two basic families. The fundamental difference is that the easy direction of magnetization may be either the basal plane of the crystal or the hexagonal axis. These are referred to as planar or uniaxial ferrites respectively. Because of the existence of these directions of easy magnetization, large internal fields may be achieved with relatively small external fields when the external field is applied parallel to the direction of the anisotropy field. Through the proper choice of materials the bulk of the required internal field can be supplied by the anisotropy field.

A sample of an uniaxial oriented ferrite was obtained from Sperry Microwave Electronics Company. This material, designated A-127, has the following characteristics:

$$4\pi M_s = 3500 \text{ gauss}$$
$$\Delta H = 1900 \text{ oersteds}$$
$$H_a = 9500 \text{ oersteds}$$
$$\epsilon_r = 14$$
$$\tan \delta = 0.002$$
$$T_c \sim 450^{\circ}C$$
$$g = 1.92.$$

Unfortunately, the only available shape for A-127 was an elliptical disc approximately 1 inch x 0.6 inch x 0.2 inch thick, having the direction of easy magnetization parallel to the minor axis. In the reciprocal phase shifter, a rod geometry with a longitudinal magnetic field is required. A test sample was made by cutting segments from the disc parallel to the minor axis and gluing them end to end. The result is a rod with the direction of easy magnetization along its axis. The photograph, Figure 13, clearly shows the many pieces that were necessary to make this first sample.

In the experimental program the object was to determine a ferrite geometry (cross-section) and position in the waveguide which would result in an optimum figure of merit for a phase shifter. The figure of merit is a function of the rod cross section, the orientation and position in the waveguide, and the proximity of operation to ferromagnetic resonance. With respect to the latter variable, it is important to note that resonance in A-127 occurs theoretically at 31.5 Gc with zero magnetic field.

A series of phase shift and insertion loss measurements was made on the test piece of A-127, using a waveguide bridge setup. A block diagram of the instrumentation is given in Figure 14. As a result of an observed hysterisis effect, the measurements were made starting at the maximum available magnetic field to insure saturation of the sample. Phase shift and loss data were taken as the field was decreased through zero to the maximum available field in the opposite direction. The direction of the field variation was then reversed, and a second set of measurements was made retracing the field through the values of the first set. With each set of data the direction of the field variation is specified as either ±Z direction, which refers to the direction of propagation in the waveguide. The direction of propagation with regard to magnetic saturation has no physical significance; it serves as a reference only. Figures 15, 16, 17, and 18 show the results of these measurements, using a ferrite

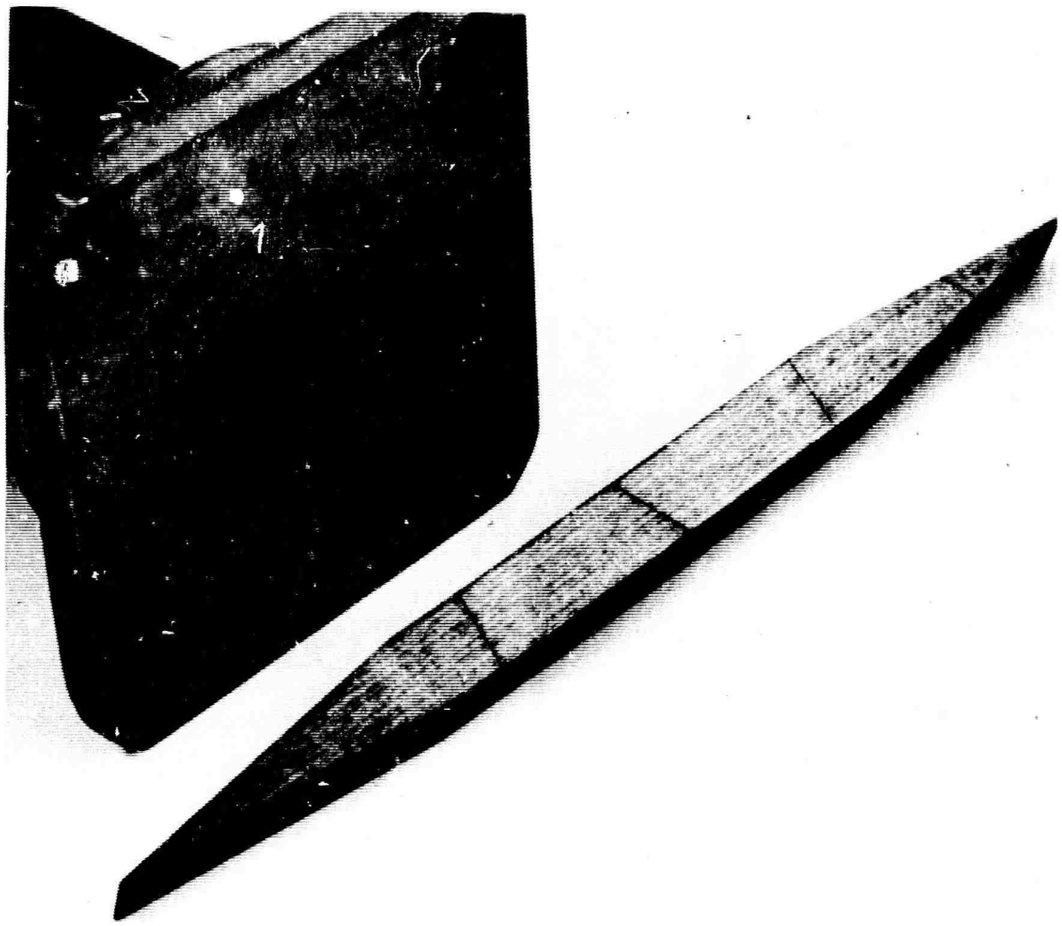

FIG. 13 - PHOTOGRAPH OF THE FABRICATED ROD OF ORIENTED UNIAXIAL FERRITE, SPERRY, A-127

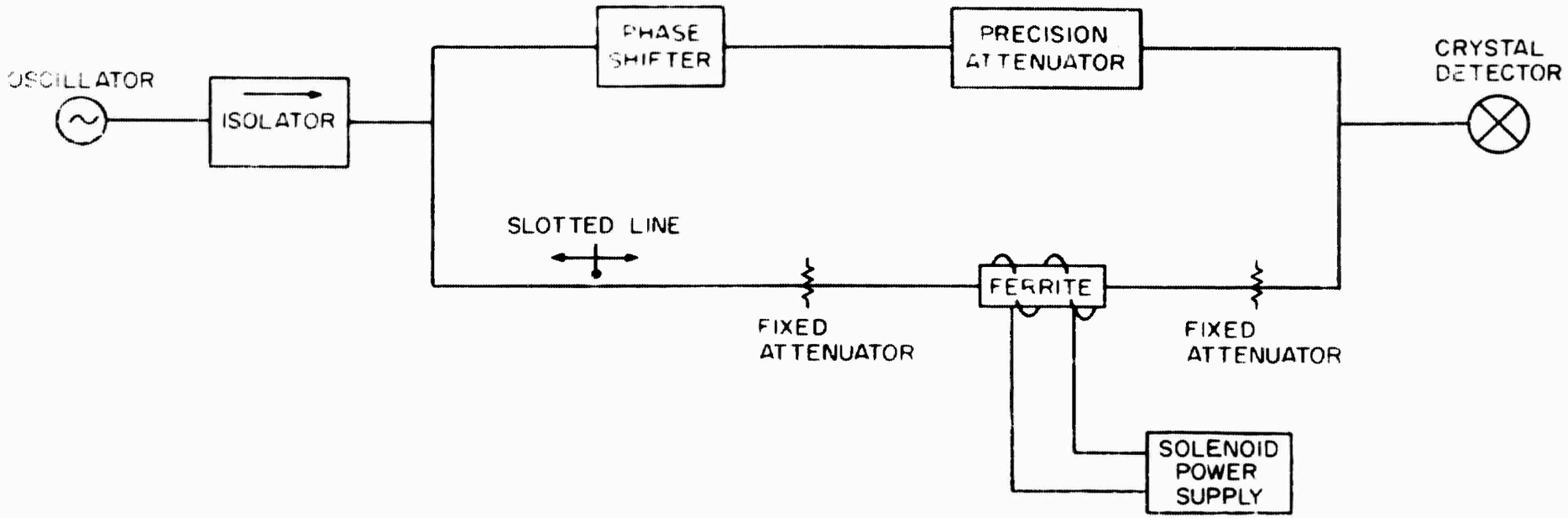

FIG. 4 – BLOCK DIAGRAM OF BRIDGE USED TO MEASURE PHASE SHIFT AND CHANGE IN INSERTION LOSS.

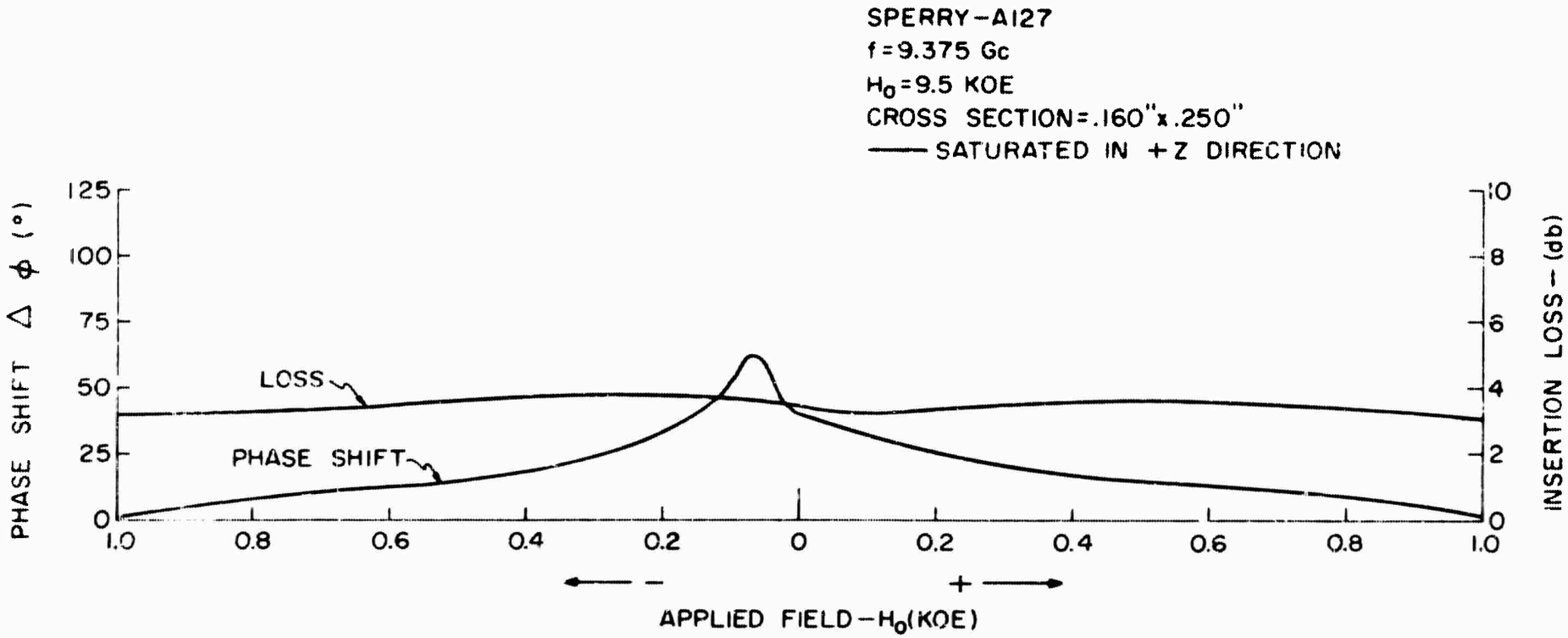

FIG. 15 - INSERTION LOSS AND PHASE SHIFT - CROSS SECTION .160"x.250" - 9.375Gc.

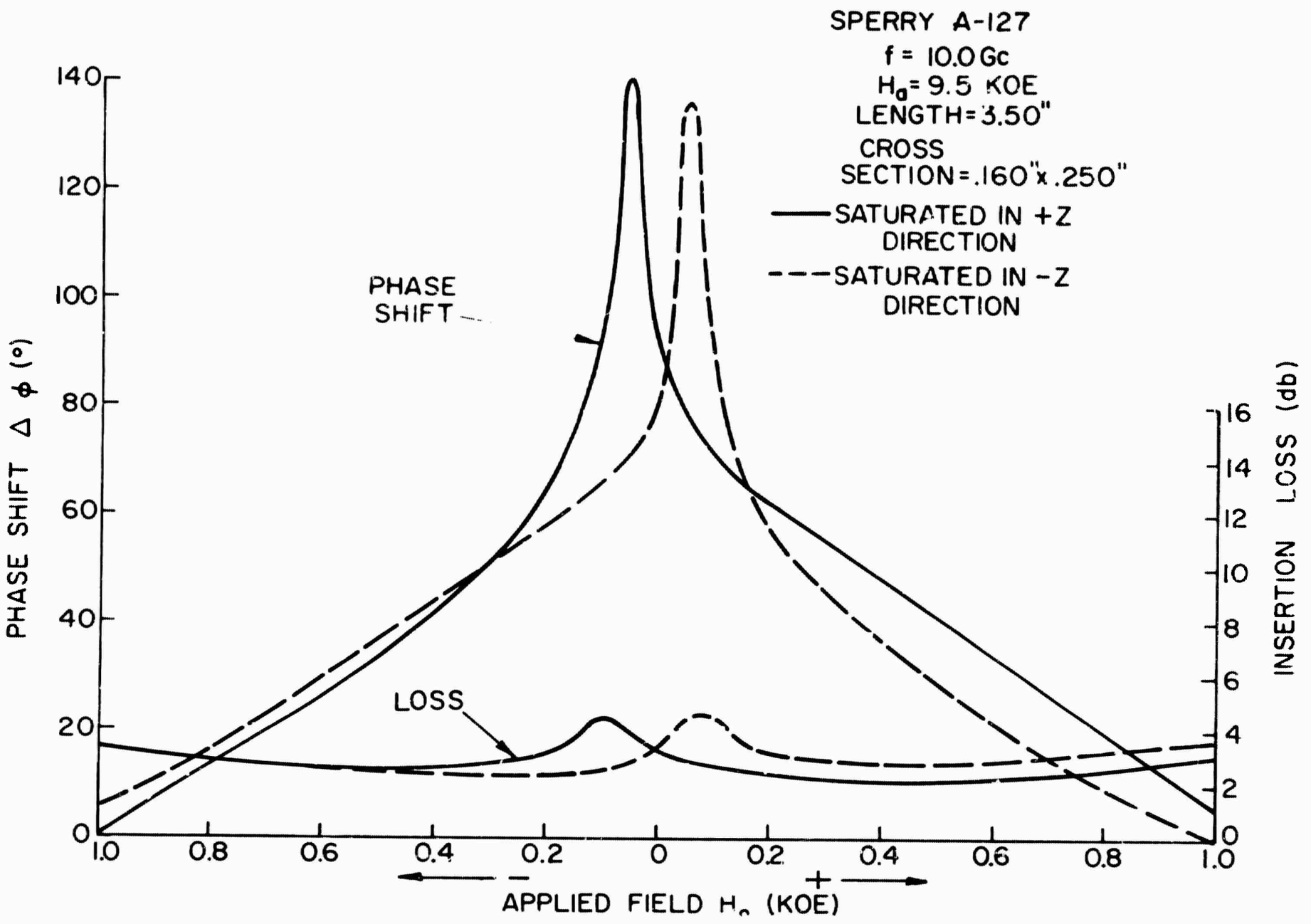

FIG. 16 - INSERTION LOSS AND PHASE SHIFT - CROSS SECTION .160" x .250" - 10.0 Gc

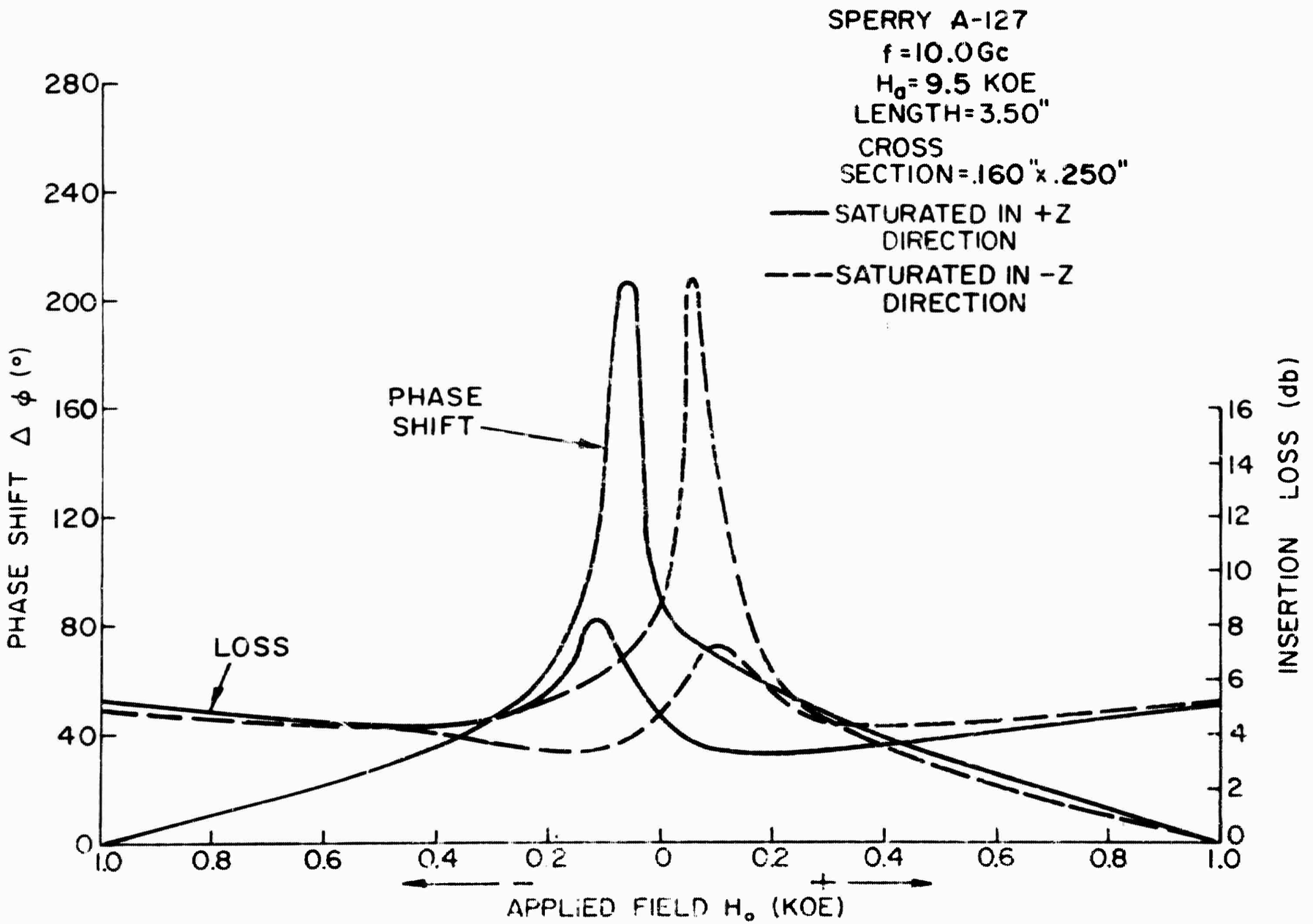

FIG. 17 – INSERTION LOSS AND PHASE SHIFT – CROSS SECTION .160" x .250" – 11.0 Gc

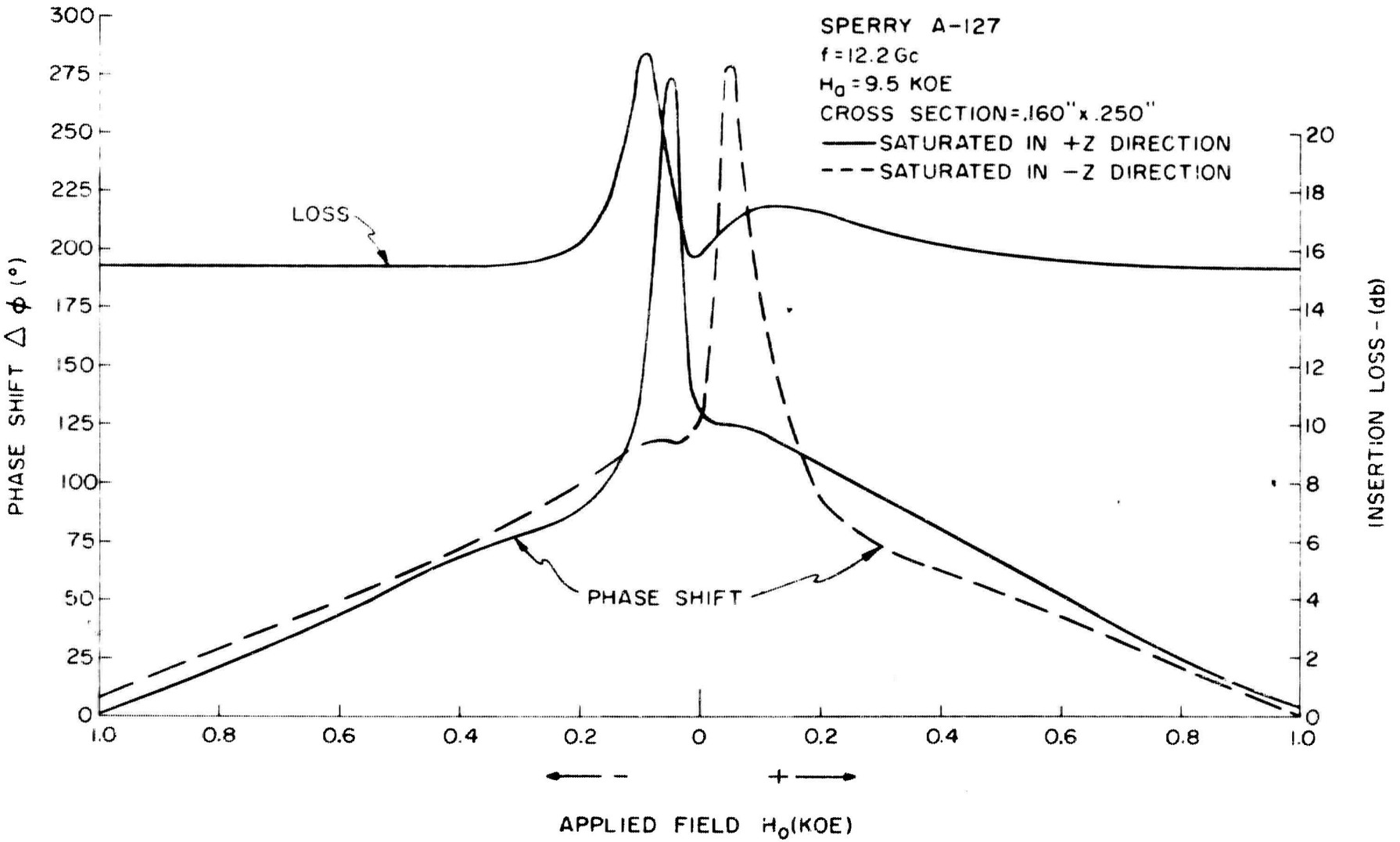

FIG. 18 – INSERTION LOSS AND PHASE SHIFT – CROSS SECTION .160" x .250" – 12.2 Gc

3.5 inches long with a 0.250 inch x 0.160 inch cross section at 9.375 Gc, 10 Gc, 11 Gc, and 12.2 Gc. The curves indicate that the greatest change in phase shift occurs for small changes in applied field close to zero internal field. The large phase shift and high loss near zero field are due to incomplete magnetic saturation. The application of a small field induces a large H_a and, hence, a large change in permeability, $\mu = \mu' + j\mu''$. The sample was positioned in the center of the waveguide with its wide dimension parallel to the broad wall of the guide. This arrangement was found to be best for the range of cross sections tested. The increasing frequency has two basic effects on phase shift and insertion loss. The binding, and hence the interaction, of the electromagnetic energy with the sample is related to the cross section dimensions and frequency. As frequency increases, more interaction takes place; and both phase shift and insertion loss increase. Also, as frequency increases, the proximity to resonance increases. This results in increased magnetic losses due to an increase in the dissipative part (μ'') of the complex permeability and increased phase shift due to the greater rate of change ($\Delta\mu'$) of the dispersive part of the complex permeability. Because the two effects tend to produce the same result, it is difficult to determine which effect is predominant. Measurements made from 10 Gc to 12.2 Gc showed that insertion loss and phase shift increase as expected. The figure of merit decreased slightly over this small frequency interval. This decrease is in agreement with an analysis which was completed after these measurements were made (see Appendix A of this report). From the generalized curves of χ' and χ'' (Figures A-1 and A-2) theoretical curves of μ' and μ'' have been constructed for the test material over this range of frequencies, and they are shown in Figure 19. The predicted figure of merit which is proportional to $\frac{\Delta\mu'}{\mu''}$, is found to decrease as frequency increases, as is shown in Figure 19. The results of the measurements at 9.375 Gc, however, are not in agreement with this trend since the loss figure did not decrease from 10 Gc to 9.375 Gc.

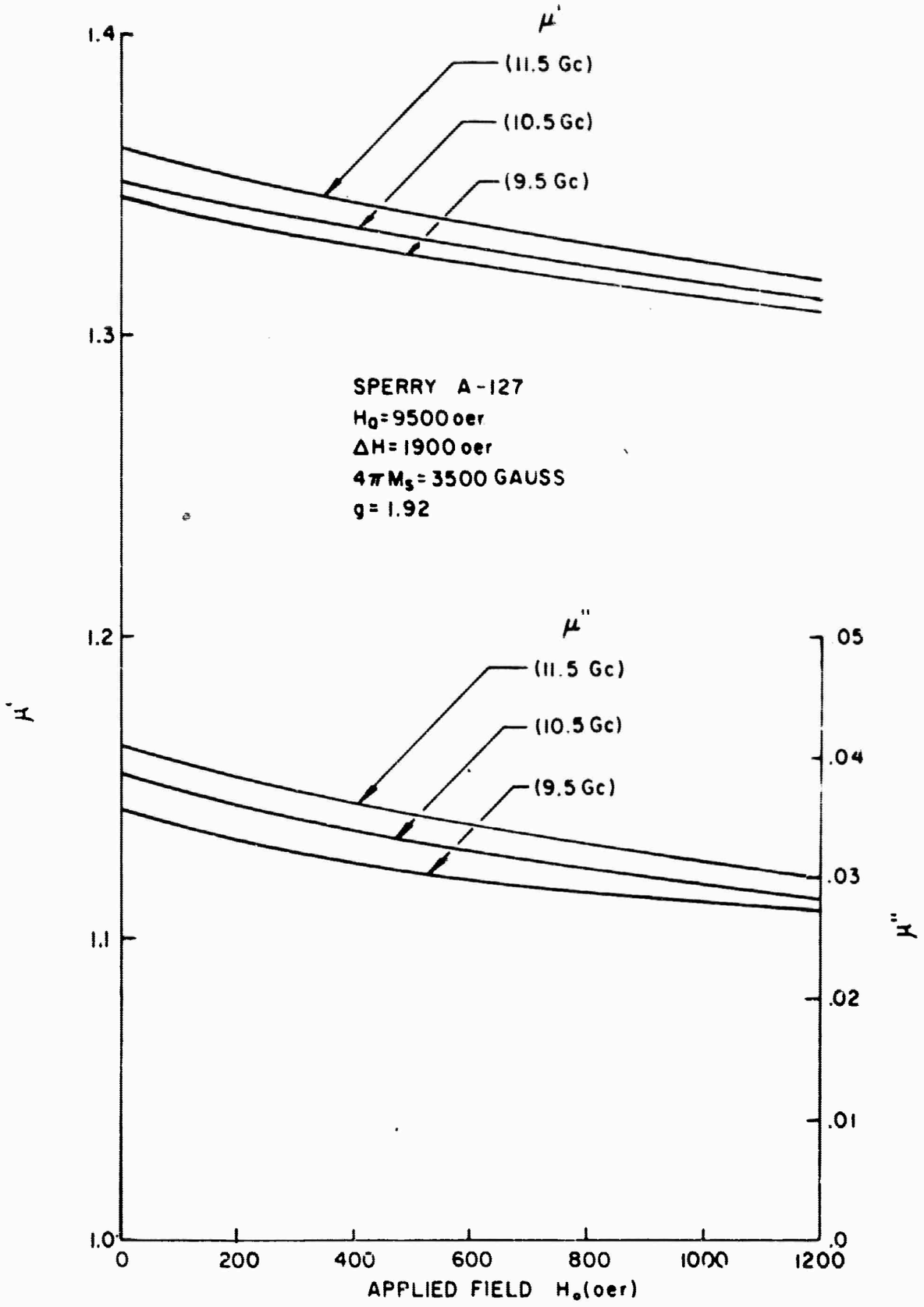

FIG. 19 - μ' AND μ'' vs APPLIED FIELD FOR SPERRY A-127

This behavior is not understood. In Figure 20, measured data is given for a ferrite cross section of 0.160 inch x 0.160 inch at 12.2 Gc. On comparing this data with Figure 18, one may observe that the reduction in cross section resulted in less phase shift and lower loss; however, the figure of merit did not change appreciably. This indicates that the activity has not been altered, and hence the reduction in both phase shift and loss is due to the weaker binding. Measurements were performed with a ferrite cross section of 0.075 inch x 0.160 inch at K-band. The results are given in Figures 21 and 22 for 18.55 Gc and 25 Gc. Since the generalized curves given in the Appendix, have not yet been extended to cover this region, a computation was performed which showed that the figure of merit should decrease with increasing frequency as observed. This shows that the measured figure of merit and the computed ratio of $\frac{\Delta\mu'}{\mu''}$, which is a measure of the bulk magnetic properties, behaved as expected. Examination of the individual values of $\Delta\mu'$, however, leads to the prediction of a larger phase shift at 25 Gc. It is felt that there may be a measurement error due to a more complicated mode being set up in the K-band guide by the ferrite. The properties of the postulated new mode might result in less interaction with the ferrite; however, since this also would reduce loss the figure of merit should be unchanged.

Further measurements were performed for cross sections of 0.200 inch x 0.250 inch, 0.160 inch x 0.250 inch, 0.160 inch x 0.160 inch, 0.100 inch x 0.160 inch, and 0.075 inch x 0.160 inch; and there was no substantial increase in the figure of merit as expected. At magnetic fields far above resonance, generalized curves of χ' and χ'' indicate that, μ' does not change very fast with changes in material characteristics ($4\pi M_s$, ΔH, and H_a). However, μ'' is affected by these characteristics; thus, the figure of merit, $\frac{\Delta\mu'}{\mu''}$, can be improved by choosing more favorable materials. A good figure of merit cannot be achieved above resonance for the Sperry A-127 material because

FIG. 20 – INSERTION LOSS AND PHASE SHIFT – CROSS SECTION .160" x .160" – 12.2 Gc

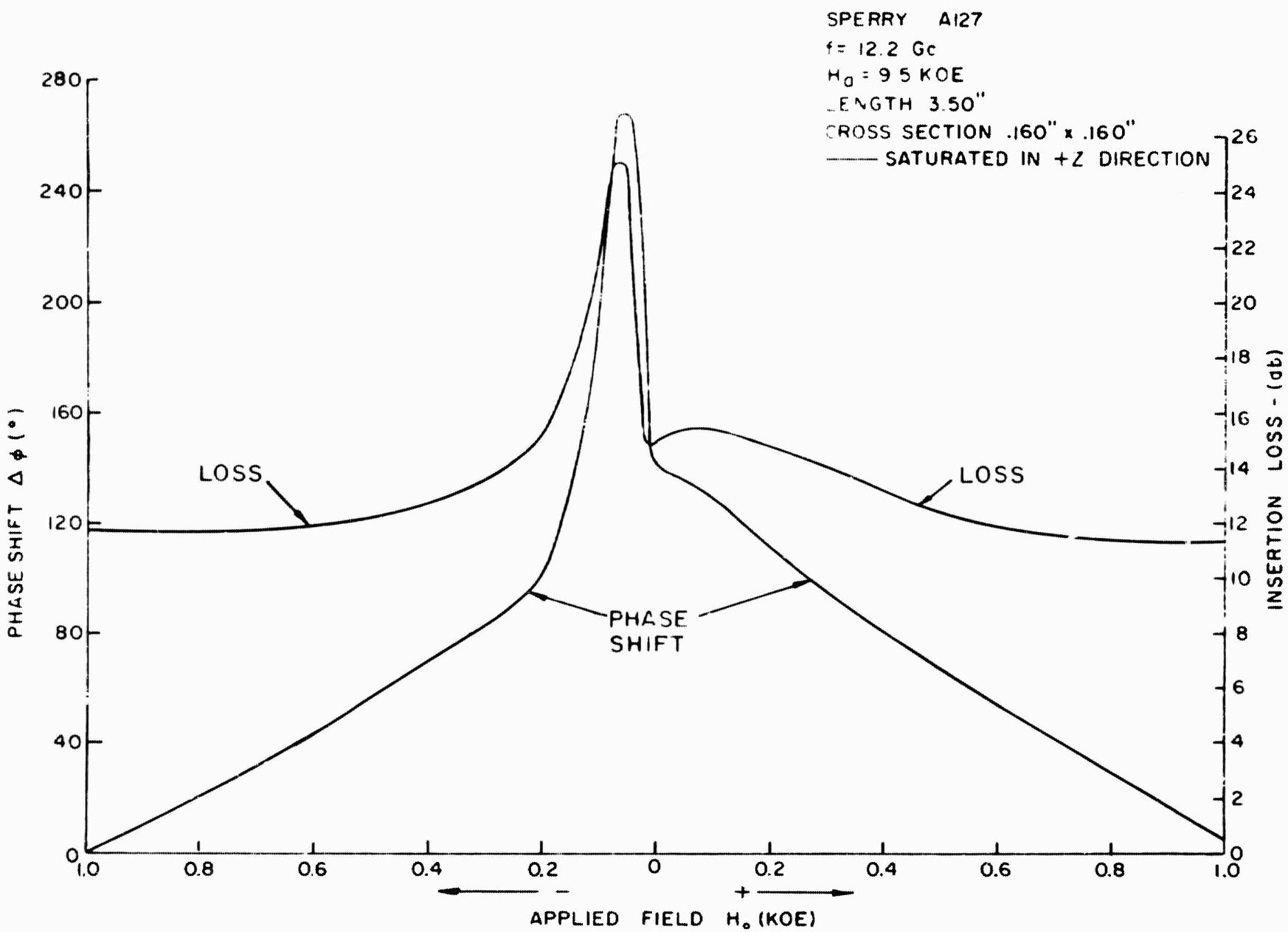

FIG. 20 – INSERTION LOSS AND PHASE SHIFT – CROSS SECTION .160" x .160" – 12.2 Gc

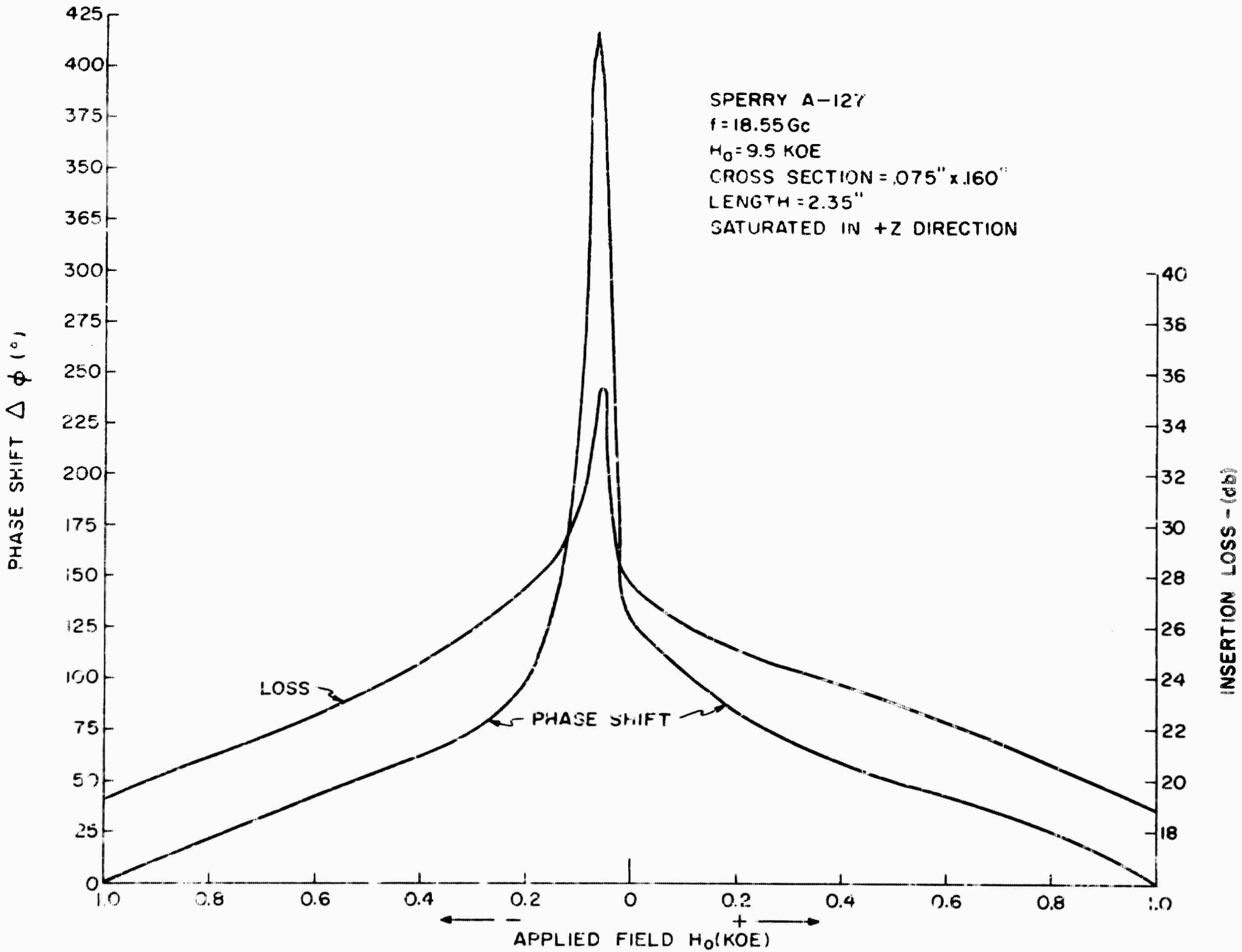

FIG.21 — INSERTION LOSS AND PHASE SHIFT — CROSS SECTION .075" x .160" — 18.55 Gc

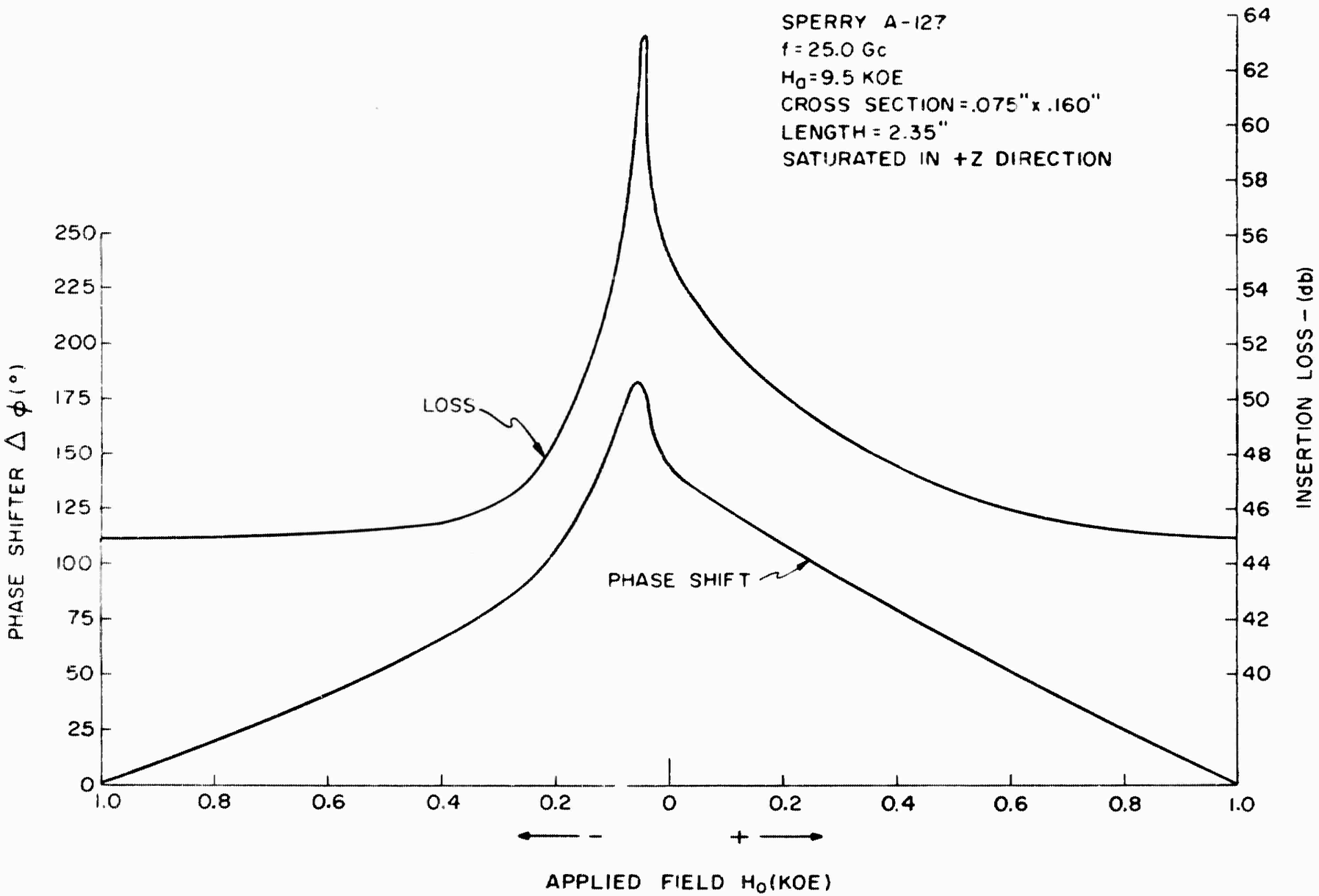

FIG. 22 – INSERTION LOSS AND PHASE SHIFT – CROSS SECTION .075" x .160" – 25Gc

of its large linewidth, $\Delta H = 1900$ oersteds. The greatest improvement in figure of merit is achieved by a reduction in linewidth. Using the generalized curves, one may construct curves of μ' and μ'' versus applied field for different values of H_a and ΔH as shown in Figures 23 through 28. Fictitious negative values of H_o have been allowed in order to see the resonance curve shape. The figure of merit, which was computed for an applied field variation of 0 to 1000 oersteds for the data in Figures 23, 24, and 25 shows no substantial change as H_a changes from 11.2 K oersteds to 5.0 K oersteds to 3.5 K oersteds. However, Figures 26, 27, and 28 show that as the linewidth was reduced from 2000 oersteds through 100 oersteds, a substantial improvement was realized. Based on the analysis, it is felt that the uniaxial anisotropic ferrites would not be well suited for operation above resonance since they are characterized by large linewidths.

Planar anisotropic ferrites have achieved linewidths of the order of 150 oersteds.[8, 9] Using this value of linewidth, one could determine an optimum material for operation above resonance by solving for the H_a which gives the greatest $\frac{\Delta\mu'}{\mu''}$.

During the third quarter a sample of planar material will be secured and measurements similar to those described in this section will be conducted.

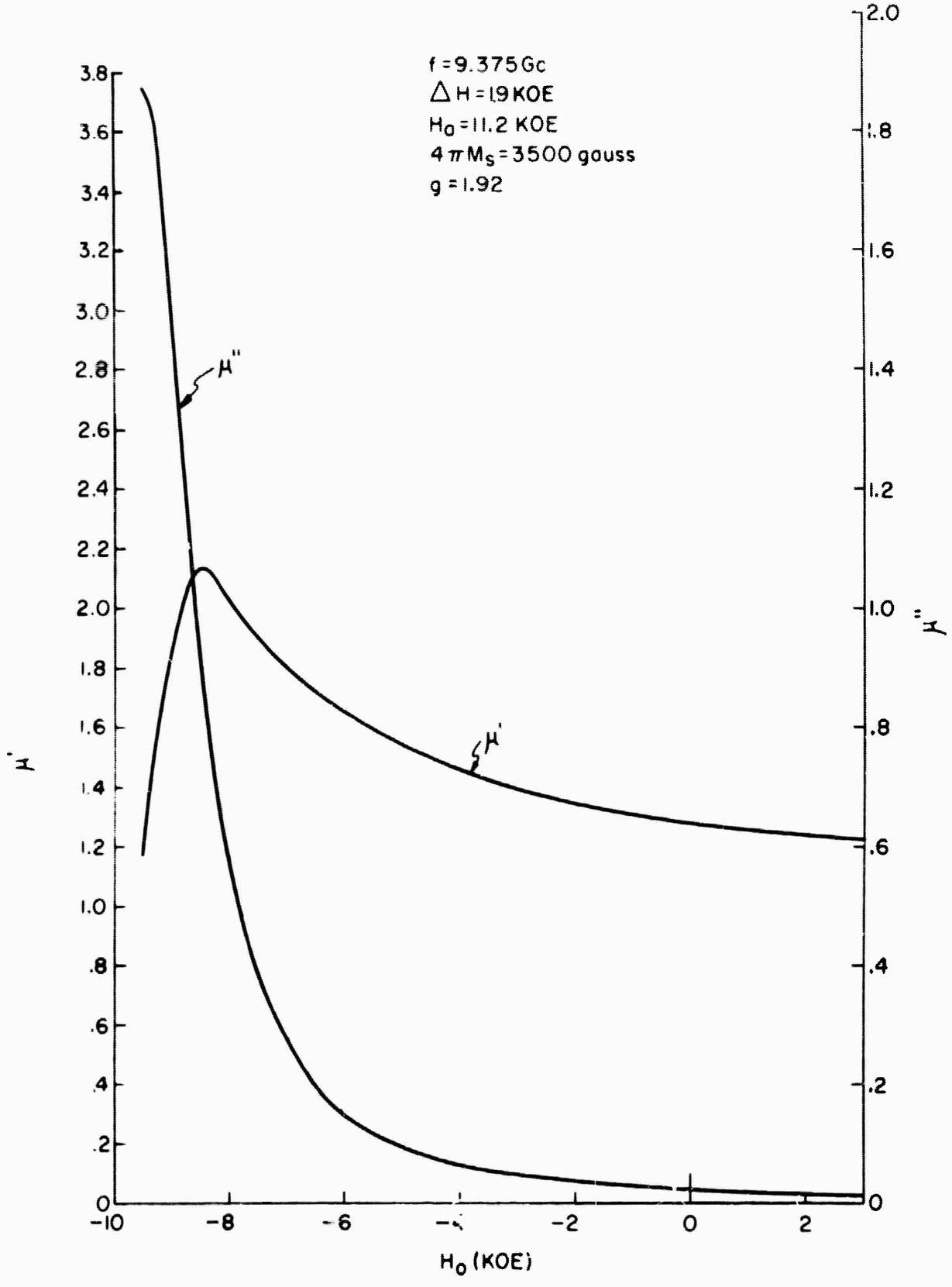

FIG. 23 – μ' AND μ'' vs APPLIED FIELD, H_0 = 11.2 KOE AND ΔH = 1.9 KOE

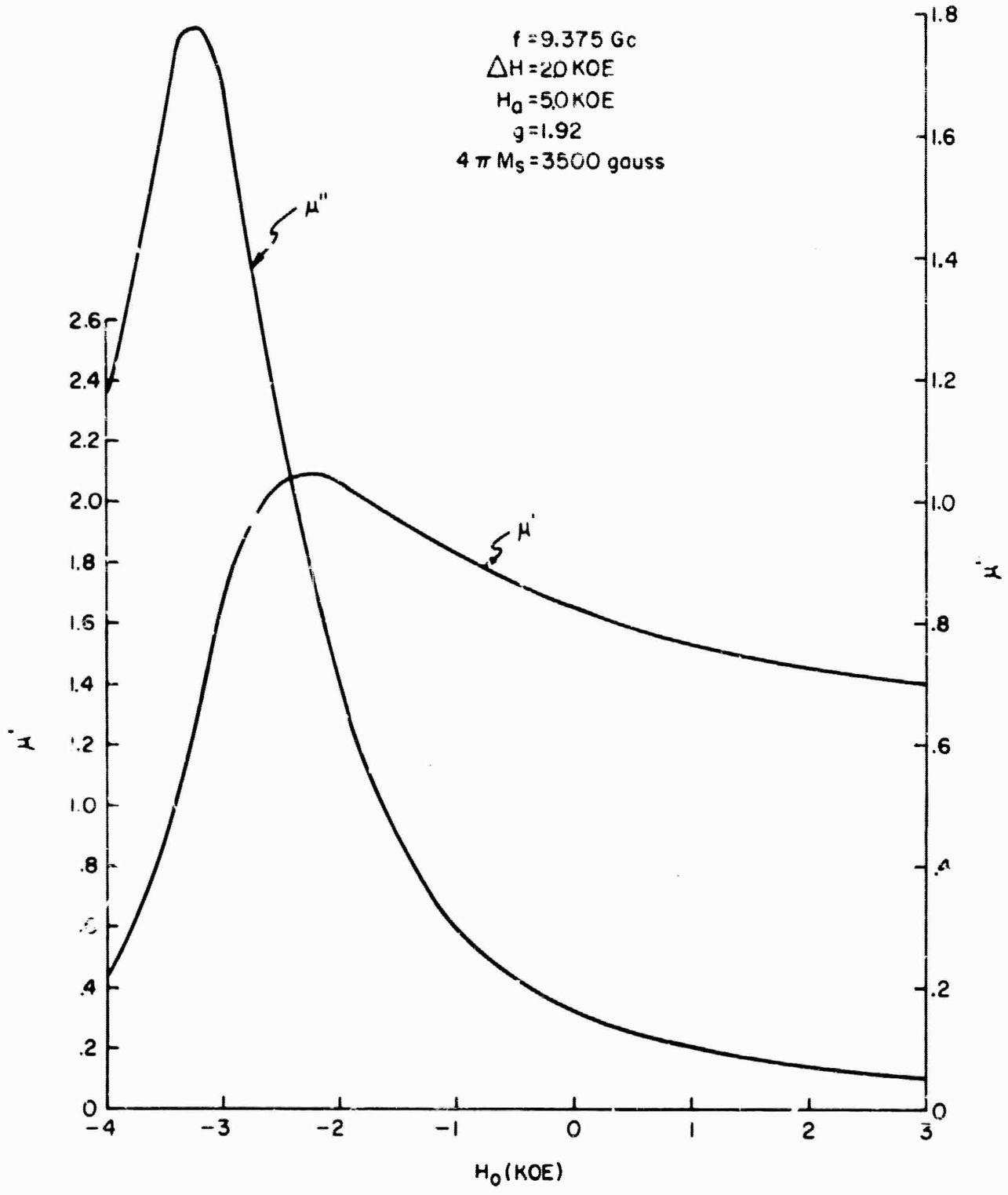

FIG. 24 – μ' AND μ'' vs APPLIED FIELD, H_0 = 5.0 KOE AND ΔH = 2.0 KOE

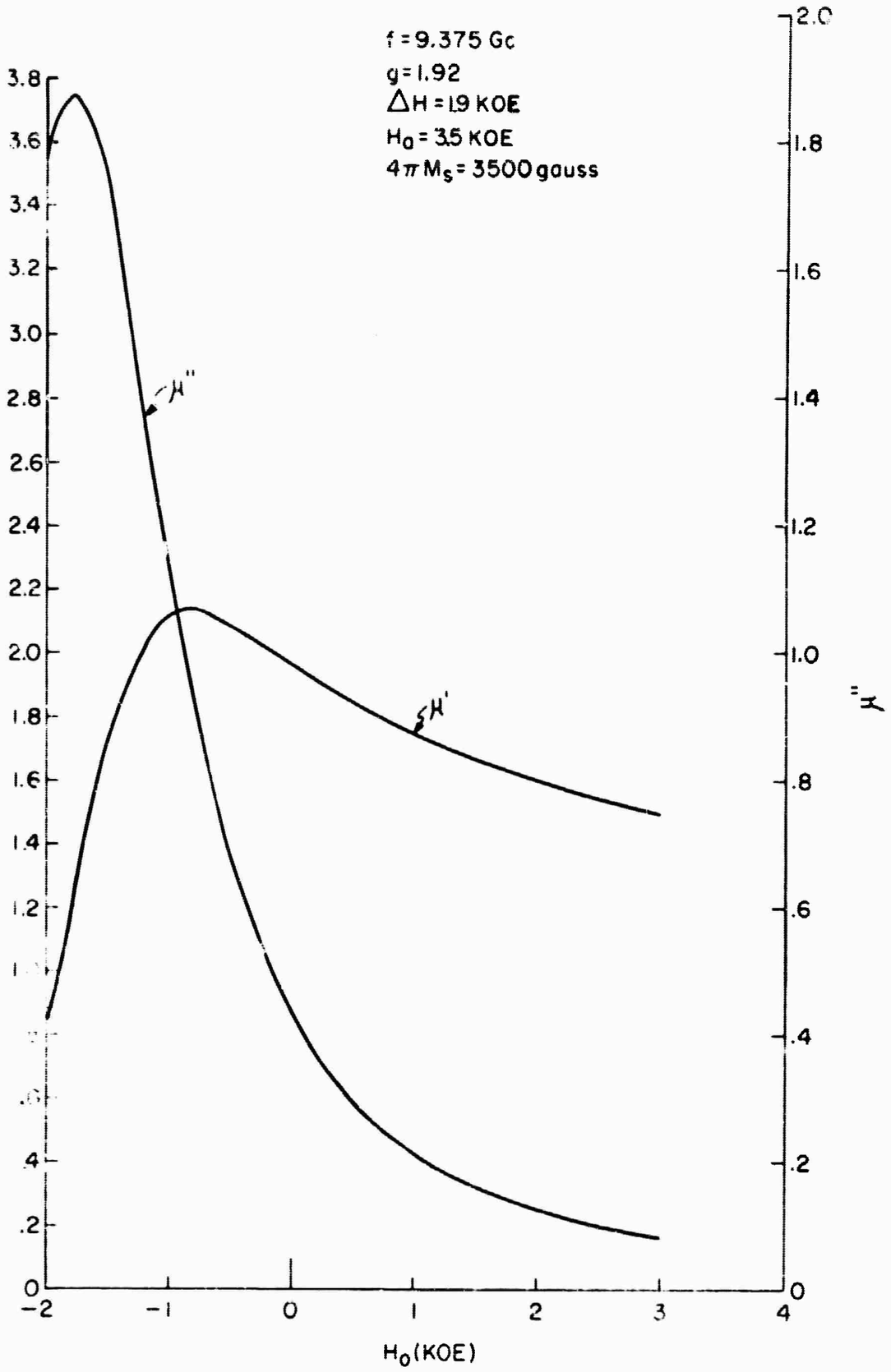

FIG. 25 - μ' AND μ'' vs APPLIED FIELD, H_0 = 3.5 KOE AND ΔH = 1.9 KOE

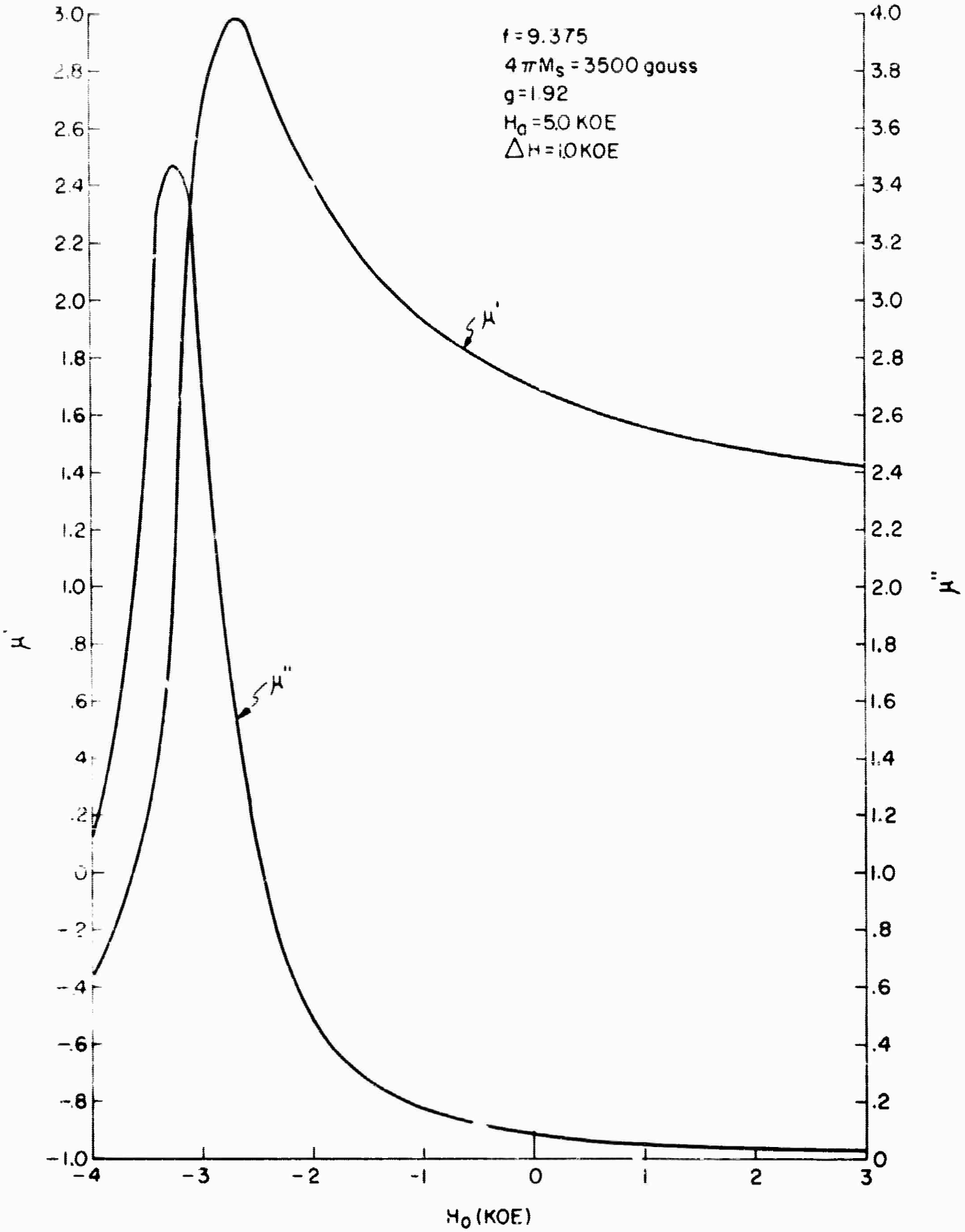

FIG. 26 – μ' AND μ'' vs APPLIED FIELD, $H_0 = 5.0$ KOE AND $\Delta H = 1.0$ KOE

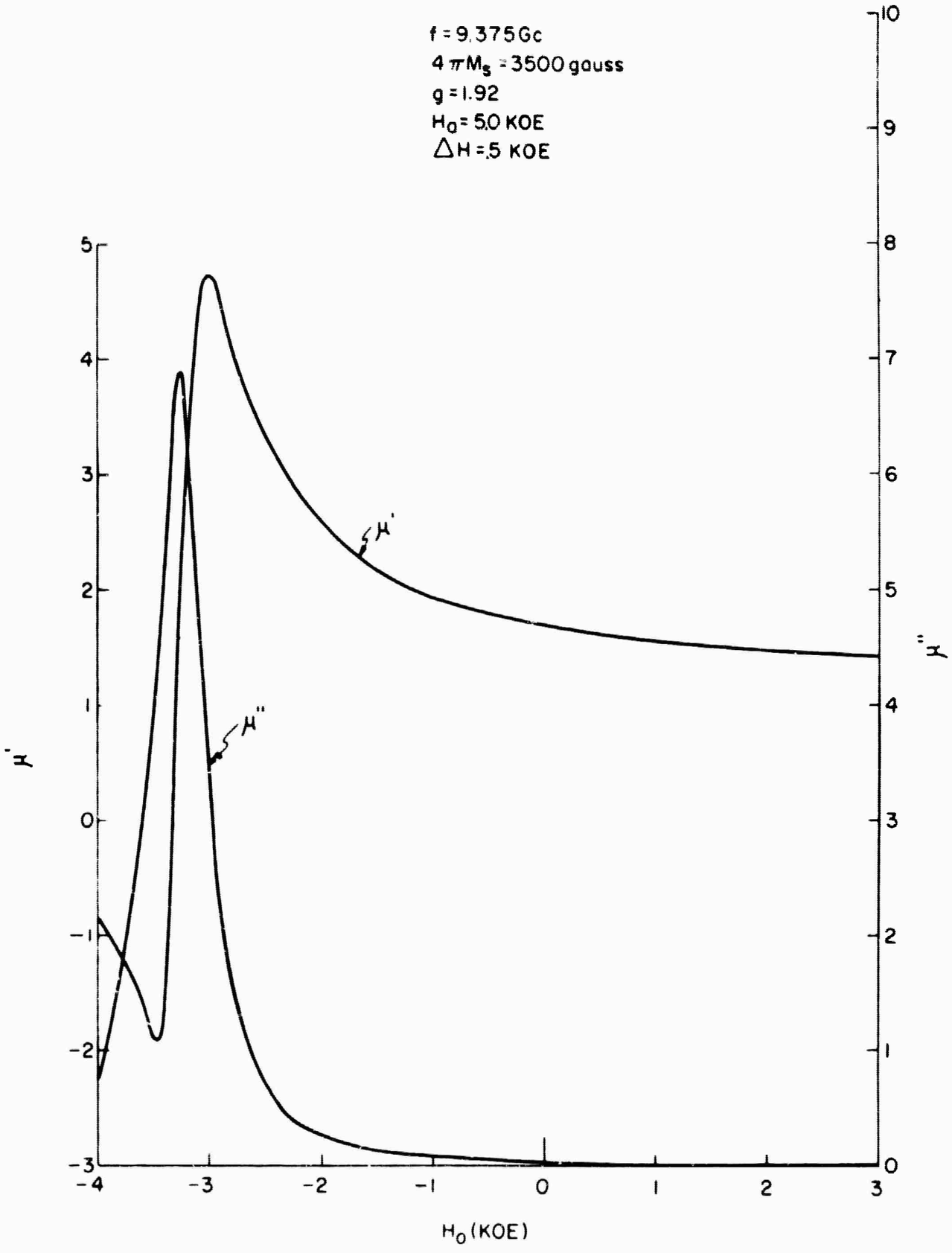

FIG. 27 $-\mu'$ AND μ'' vs APPLIED FIELD, H_0 = 5.0 KOE AND ΔH = .5 KOE

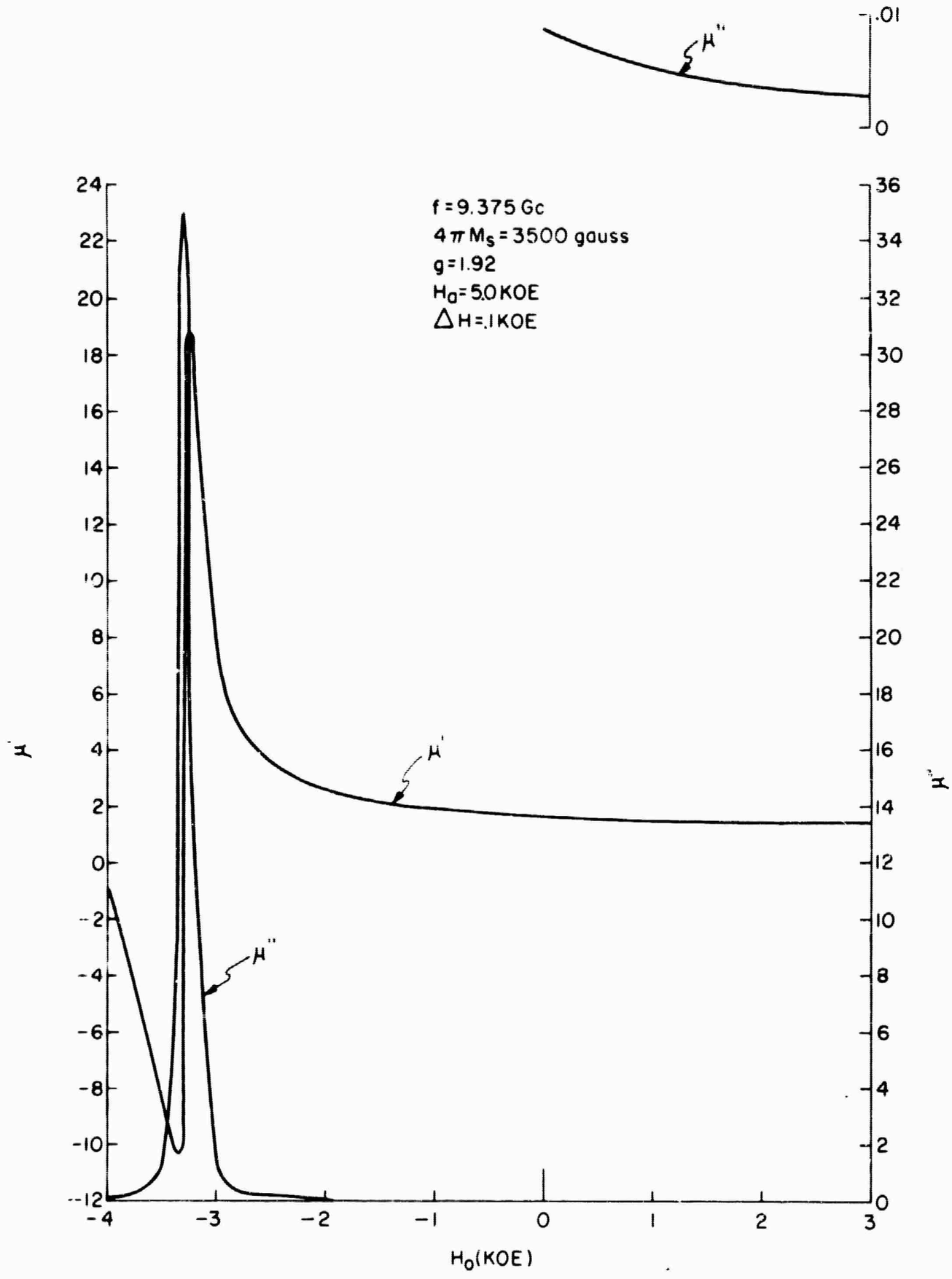

FIG. 28 – μ' AND μ'' vs APPLIED FIELD, H_o = 5.0 KOE AND ΔH = .10 KOE

V. CONCLUSIONS

The experimental investigation into the characteristics of ferrite rods, operated with longitudinal magnetic fields above ferromagnetic resonance, has shown that none of the materials tested would be satisfactory for the proposed phase shifter. A theoretical analysis, which was carried out at the same time, has been applied to show that the phase shift and loss characteristics are what would be expected for the materials tested, and that prohibitively large dynamic fields would be needed to realize a figure of merit of 360 degrees per db. The analysis sets forth a narrow ferromagnetic linewidth as the principle requirement for a high figure of merit with realistic ranges of dynamic magnetic field. Presently available polycrystalline materials have linewidths greater than 100 oersteds and do not satisfy this requirement; however, experiments at Trans-Tech with copper doping of a nickel-zinc ferrite are expected to result in polycrystalline material with a linewidth on the order of 50 oersteds. A completely satisfactory figure of merit is not predicted for this material but a definite trend for improvement should be demonstrated. Narrower linewidths are available in single crystal ferrites, and a search for a source of large size single crystals needed for the subject phase shifter is presently being made.

A further important material characteristic is a large saturation moment to alleviate the need for high magnetic bias fields. Presently available materials are limited to saturation moments less than 5000 oersteds; thus, fields on the order of 1200 oersteds are needed for X-band operation. For smaller bias fields, materials having an oriented anisotropy field parallel to the applied field are required. Unfortunately, the linewidth of the uniaxial ferrites studied thus far are quite large and a poor figure of merit was experienced. Single crystal planar ferrites have been grown with measured linewidths of 18 oersteds; however, at the present state-of-the-art, the probability

of early availability of large single crystals of oriented ferrites is not known.

At C-band, materials with saturation moments greater than 3000 oersteds would be satisfactory with regard to minimizing the bias field. Single crystal lithium ferrite offers both narrow linewidth (4 oersteds), and high saturation moment ($4\pi M_s \approx 3600$). A search for a source of large crystals of lithium ferrite in either single crystal or aggregate form is presently being made. If the search is successful, a phase shifter with a satisfactory figure of merit may be realized for C-band operation.

The cross-sectional dimensions of the ferrite must be decreased to the point where body resonances are suppressed. It is anticipated, however, that the waveguide associated with the ferrite must be reduced correspondingly if phase shift activity is to be maintained.

A second approach to the suppression of body resonances is to totally fill a waveguide structure. Several advantages are thus realized. First, the structure lends itself to theoretical analysis and second, a practical consideration, the accompanying reduction in waveguide size lends itself to reduced drived coil inductance and hence to reduced driver energy.

It could be pointed out here that further considerations are being given to an ultimate design of the phase shifter with emphasis on efficient utilization of the driver energy. The prospect of reducing the length of the magnetic circuit by folding the RF structure is particularly attractive.

Since the survey of materials has been extended to include single crystal ferrites, the contractor feels that it is desirable to bring to bear the technology of solid state physics.

REFERENCES

1. J. Smit and H P J Wijn, Ferrites, John Wiley and Sons Inc., New York, Chapter IV; 1959.

2. G P Rodrigue, "Magnetic Materials for Millimeter Wave Applications," IRE Trans., Vol MTT-11, pp. 351-356; September 1963.

3. G P Rodrigue, "Theoretical and Experimental Investigation to Determine the Microwave Characteristics and Applications of Hexagonal Magnetic Oxides to Microwave Circuitry " Sperry Microwave Electronics Co., Clearwater, Fla., Tech. Report on Contract No. AF 30(602)-2330; December 10, 1961.

4. D J DeBitetto, F K du Pré and F G Brockman, "Hexagonal Magnetic Materials for Microwave Applications," Philips Laboratories, Irvington-on-Hudson, New York, Final Report on Contract No. DA 36-039-SC-85279, July, 1961

5 D C Stinson, "Ferrite Line Width Measurements in a Cross-Guide Coupler," IRE Trans , Vol MTT-6, pp. 446-450; October 1958.

6. W Viehmann, "Ferromagnetic Resonance Experiments on Crystal-Oriented Hexagonal Ferrites," Harry Diamond Lab., Army Materiel Command, Washington 25, D C TR-1227, p. 13; May 8, 1964

7. J E Pippin and C L Hogan, "Resonance Measurements on Nickel-Cobalt Ferrites as a Function of Temperature and on Nickel Ferrite-Aluminates " IRE Trans., Vol MTT-6, pp. 77-82; January, 1958

8. I Bady and G McCall, "Ferromagnetic Line Width of Nonoriented Polycrystalline Hexagonal Ferrites with Large Magnetic Anisotropy Fields," IEEE Trans., Vol. MTT-1, No. 5, pp. 442-443; September, 1963.

9. R. Harvey, I. Garden and R. Braden, "Hexagonal Magnetic Compounds," RCA Laboratories, Princeton N J., Quarterly Rept. No 6, Contract DA 36-039 sc 87533; December, 1962.

APPENDIX A

An analysis was performed to determine the most general form of the complex susceptibility.[1,2] This included the consideration of demagnetizing factors, loss, and anisotropy effects. The analysis follows the well established form and is intended to express the dispersive and dissipative parts of the susceptibility as generalized curves which will facilitate the study of materials with varying characteristics ($4\pi M_s$, H_a, ΔH). In the first approximation, only small signal levels are considered.

The equation of motion of the total magnetization $\vec{M}$ is given by

$$\dot{\vec{M}} = \gamma(\vec{M} \times \vec{H}_{eff}) - \frac{\alpha}{|\vec{M}|} (\vec{M} \times \dot{\vec{M}}) , \qquad (A-1)$$

where the last term is the Landau-Lifshitz damping term to the first power in the damping factor α. The magnetization and effective magnetic fields are given by

$$\vec{M} = \vec{M}_o + \vec{m}\, e^{j\omega t} , \qquad (A-2)$$

and

$$\vec{H}_{eff} = \vec{H}_i + \vec{h}\, e^{j\omega t} , \qquad (A-3)$$

where $\vec{m}$ and $\vec{h}$ are contributions due to the applied RF field. Substitute Equations A-2 and A-3 into A-1.

$$\frac{d}{dt}[\vec{M}_o + \vec{m}\, e^{j\omega t}] = \gamma[(\vec{M}_o + \vec{m}\, e^{j\omega t}) \times (\vec{H}_i + \vec{h}\, e^{j\omega t})]$$

$$- \frac{\alpha}{|\vec{M}_o + \vec{m}\, e^{j\omega t}|} [(\vec{M}_o + \vec{m}\, e^{j\omega t}) \times \frac{d}{dt} (\vec{M}_o + \vec{m}\, e^{j\omega t})] .$$

Noting that

$$\frac{d}{dt}\ \vec{M}_o = 0,$$

and

$$|\vec{M}_o + \vec{m}\, e^{j\omega t}| \approx M_o \text{ since } M_o >> m \text{ for small signal levels.}$$

Equation A-4 reduces to

$$\frac{d}{dt}(\vec{m}\, e^{j\omega t}) = \gamma\,[(\vec{M}_o + \vec{m}\, e^{j\omega t}) \times (\vec{H}_i + \vec{h}\, e^{j\omega t})]$$

$$- \frac{a}{M_o}\,[(\vec{M}_o + \vec{m}\, e^{j\omega t}) \times \frac{d}{dt}\ (\vec{m}\, e^{j\omega t})]\ , \qquad \text{(A-5)}$$

$$j\omega \vec{m}\, e^{j\omega t} = \gamma\,[(\vec{M}_o \times \vec{H}_i) + (\vec{M}_o \times \vec{h}\, e^{j\omega t}) + (\vec{m}\, e^{j\omega t} \times \vec{H}_i)$$

$$+ (\vec{m}\, e^{j\omega t} \times \vec{h}\, e^{j\omega t})] - \frac{a}{M_o}\,[(\vec{M}_o \times j\omega \vec{m}\, e^{j\omega t}) + (\vec{m}\, e^{j\omega t} \times j\omega \vec{m}\, e^{j\omega t})]\ .$$

(A-6)

Neglecting terms higher than the first power in the small quantities m and h and noting that $\vec{M}_o \times \vec{H}_i = 0$ since $\vec{M}_o \,//\, \vec{H}_i$, Equation A-6 reduces to

$$j\omega \vec{m} = \gamma\,[(\vec{M}_o \times \vec{h}) + (\vec{m} \times \vec{H}_i)] - \frac{j\omega a}{M_o}\ (\vec{M}_o \times \vec{m}). \qquad \text{(A-7)}$$

Operate on Equation A-7 with $\times \vec{H}_i$,

$$j\omega \vec{m} \times \vec{H}_i = \gamma(\vec{M}_o \times \vec{h}) \times \vec{H}_i + \gamma(\vec{m} \times \vec{H}_i) \times \vec{H}_i - \frac{j\omega a}{M_o}\,(\vec{M}_o \times \vec{m}) \times \vec{H}_i\ .$$

(A-8)

This has the form, $(\vec{A} \times \vec{B}) \times \vec{C} = (\vec{C} \cdot \vec{A})\,\vec{B} - (\vec{C} \cdot \vec{B})\,\vec{A}$,

$$j\omega \vec{m} \times \vec{H}_i = \gamma(\vec{H}_i \cdot \vec{M}_o)\,\vec{h} - \gamma(\vec{H}_i \cdot \vec{h})\,\vec{M}_o + \gamma(\vec{H}_i \cdot \vec{m})\,\vec{H}_i - \gamma(\vec{H}_i \cdot \vec{H}_i)\,\vec{m}$$

$$- \frac{j\omega a}{M_o}\,[\,(\vec{H}_i \cdot \vec{M}_o)\,\vec{m} - (\vec{H}_i \cdot \vec{m})\,\vec{M}_o\,]\ . \qquad \text{(A-9)}$$

The internal field, $\vec{H}_i$, can be written as a sum of an applied field, $\vec{H}_o$, an anisotropy field, $\vec{H}_a$, and any demagnetizing field, $\vec{H}_D$.

$$\therefore \vec{H}_i = \vec{H}_o + \vec{H}_a - \vec{H}_D . \tag{A-10}$$

Since one is free to choose the directions of the applied field and the RF field, define

$$\vec{H}_i = (H_o + H_a - N_z 4\pi M_o)\hat{k} , \tag{A-11}$$

$$\vec{h} = (h_x - N_x 4\pi m_x)\hat{i} + (h_y - N_y 4\pi m_y)\hat{j} , \tag{A-12}$$

where $\hat{i}$, $\hat{j}$, and $\hat{k}$ are an orthogonal set of unit vectors. $\vec{M}_o$ is the magnetization due to $\vec{H}_i$ and $\vec{m}$ is the magnetization due to $\vec{h}$. Therefore, after saturation, $\vec{M}_o$ is in the direction of $\vec{H}_i$,

$$\vec{M}_o = M_o \hat{k} , \tag{A-13}$$

and is given by

$$\vec{M}_o = M_s \hat{k} , \tag{A-14}$$

and

$$\vec{m} = m_x \hat{i} + m_y \hat{j} . \tag{A-15}$$

In Equations A-11 and A-12, the demagnetizing field $\vec{H}_D$ has been written in terms of demagnetizing coefficients N_x, N_y and N_z, where

$$\vec{H}_D = [N] \cdot 4\pi \vec{M} , \tag{A-16}$$

which satisfies the requirement that

$$N_x + N_y + N_z = 1 . \tag{A-17}$$

From the construction of the problem, certain terms in Equation A-9 are zero:

$$\vec{H}_i \cdot \vec{h} = 0$$

$$\vec{H}_i \cdot \vec{m} = 0 \ .$$

Therefore Equation A-9 reduces to

$$j\omega\vec{m} \times \vec{H}_i = \gamma(\vec{H}_i \cdot \vec{M}_s)\,\vec{h} - \gamma(\vec{H}_i \cdot \vec{H}_i)\,\vec{m} - \frac{j\omega\alpha}{M_s}\,(\vec{H}_i \cdot \vec{M}_s)\,\vec{m} \ . \qquad \text{(A-18)}$$

Multiply both sides of Equation A-18 by γ and equate vector components.

$$j\omega\gamma H_i m_y = \gamma^2 H_i M_s (h_x - N_x 4\pi m_x) - \gamma^2 H_i^2 m_x - j\omega\alpha\gamma H_i m_x \qquad \text{(A-19)}$$

$$-j\omega\gamma H_i m_x = \gamma^2 H_i M_s (h_y - N_y 4\pi m_y) - \gamma^2 H_i^2 m_y - j\omega\alpha\gamma H_i m_y \qquad \text{(A-20)}$$

In order to simplify Equation A-19 and A-20, define

$$\gamma 4\pi M_s = \omega_M$$

$$\gamma H_i = \omega_o \ .$$

The damping factor α is given by

$$\alpha = \frac{1}{\omega T} \ ,$$

where T is the spin-lattice relaxation time. Substitute these expressions into Equations A-19 and A-20 and solve them simultaneously for m_x:

$$m_x\left[-\omega^2 + j(N_x + N_y)\frac{\omega_M}{T} + (N_x + N_y)\omega_M\omega_o + j\frac{2\omega_o}{T} + \omega_o^2 + \omega_M^2 N_x N_y - \frac{1}{T^2}\right]$$

$$= \frac{\omega_M}{4\pi}\left[-j\omega h_y + (\omega_M N_y + \omega_o + \frac{j}{T})\,h_x\right], \text{ and} \qquad \text{(A-21)}$$

$$4\pi m_x = \frac{\omega_M\left[-j\omega h_y + (\omega_o + N_y\omega_M + \frac{j}{T})\,h_x\right]}{\left[\omega_o + N_x\omega_M + \frac{j}{T}\right]\left[\omega_o + N_y\omega_M + \frac{j}{T}\right] - \omega^2} \ . \qquad \text{(A-22)}$$

The induced magnetization is related to the applied RF magnetic field through the susceptibility tensor, χ,

$$\vec{m} = [\chi] \cdot \vec{h} \quad . \tag{A-23}$$

Solving for the xx diagonal component of the susceptibility tensor in gaussian units,

$$\chi_{xx} = \frac{4\pi m_x}{h_x} \quad . \tag{A-24}$$

Therefore, from Equation A-22,

$$\chi_{xx} = \frac{\omega_M(\omega_o + N_y\omega_M + \frac{j}{T})}{[\omega_o + N_x\omega_M + \frac{j}{T}\,][\omega_o + N_y\omega_M + \frac{j}{T}] - \omega^2} \quad . \tag{A-25}$$

Equation A-25 is the most general form of the effective complex susceptibility for small signal levels.

A case of particular interest is a rod magnetized along its axis ($\hat{k}$ direction). If the rod's length is much larger than its radius, the demagnetizing coefficients are given by,

$$N_z = 0 \,,$$

and

$$N_x = N_y = \frac{1}{2} \quad .$$

Equation A-25 has the form

$$\chi_{xx} = \frac{\omega_M(\omega_o + \frac{\omega_M}{2} + \frac{j}{T})}{[\omega_o + \frac{\omega_M}{2} + \frac{j}{T}]^2 - \omega^2} \quad . \tag{A-26}$$

Let $\omega_r = \omega_o + \frac{\omega_M}{2}$.

Then it follows that:

$$\chi_{xx} = \frac{\omega_M(\omega_r + \frac{j}{T})}{[\omega_r + \frac{j}{T}]^2 - \omega^2}, \tag{A-27}$$

$$\chi_{xx} = \frac{\omega_M(\omega_r + \frac{j}{T})}{[\omega_r^2 - \omega^2 - \frac{1}{T^2}] + 2\frac{j\omega}{T}} . \tag{A-28}$$

The real and imaginary parts (the dissipative and dispersive parts, respectively) of the complex susceptibility can be found by rationalization of Equation A-28:

$$\chi_{xx} = \chi'_{xx} - j\chi''_{xx} , \tag{A-29}$$

where

$$\chi'_{xx} = \frac{\omega_M\omega_r(\omega_r^2 - \omega^2 - \frac{1}{T^2}) + 2\frac{\omega_M\omega_r}{T^2}}{(\omega_r^2 - \omega^2 - \frac{1}{T^2})^2 + 4\frac{\omega_r^2}{T^2}}, \tag{A-30}$$

and

$$\chi''_{xx} = \frac{\frac{\omega_M}{T}(\omega_r^2 + \omega^2 + \frac{1}{T^2})}{(\omega_r^2 - \omega^2 - \frac{1}{T^2})^2 + 4\frac{\omega_r^2}{T^2}} . \tag{A-31}$$

In terms of the complex permeability,

$$\mu' = 1 + \chi'_{xx} , \tag{A-32}$$

and

$$\mu'' = \chi''_{xx} . \tag{A-33}$$

In Equations A-30 and A-31, ω_r is given by

$$\omega_r = \omega_o + \frac{\omega_M}{2} = \gamma \left[H_c + H_a + 2\pi M_s \right] \quad . \tag{A-34}$$

This contains the total effect of any anisotropy field (in materials with no net anisotropy, H_a can be set equal to zero in A-34) present. The spin-lattice relaxation time T is related to the linewidth by,

$$\frac{1}{T} = \gamma \frac{\Delta H}{2} \quad . \tag{A-35}$$

The resonant frequency can be found by maximizing Equation A-31,

$$\omega_{res}^2 = -(\omega_r^2 + \frac{1}{T^2}) + 2\omega_r (\omega_r^2 + \frac{1}{T^2})^{\frac{1}{2}} \quad . \tag{A-36}$$

A general set of curves for χ' and χ'' can be found by normalizing Equations A-30 and A-31 with respect to frequency:

$$\chi'' = \frac{\frac{\omega_M}{T} (\omega_r^2 + \omega^2 + \frac{1}{T^2})}{(\omega_r^2 - \omega^2 - \frac{1}{T^2})^2 + 4\frac{\omega_r^2}{T^2}} , \tag{A-31}$$

$$\chi'' = \frac{\frac{\omega^3 \omega_M}{\omega T} \left[\left(\frac{\omega_r}{\omega}\right)^2 + \left(\frac{1}{\omega T}\right)^2 + 1 \right]^2}{\omega^4 \left[\left(\frac{\omega_r}{\omega}\right)^2 - \left(\frac{1}{\omega T}\right)^2 - 1 \right]^2 + 4\omega^4 \left(\frac{\omega_r}{\omega}\right)^2 \left(\frac{1}{\omega T}\right)^2} , \tag{A-37}$$

$$\chi'' = \frac{\omega_M}{\omega} \frac{\left(\frac{1}{\omega T}\right) \left[\left(\frac{\omega_r}{\omega}\right)^2 + \left(\frac{1}{\omega T}\right)^2 + 1 \right]^2}{\left[\left(\frac{\omega_r}{\omega}\right)^2 - \left(\frac{1}{\omega T}\right)^2 - 1 \right]^2 + 4 \left(\frac{\omega_r}{\omega}\right)^2 \left(\frac{1}{\omega T}\right)^2} , \tag{A-38}$$

$$\frac{\omega}{\omega_M}\chi'' = \frac{\left(\frac{1}{\omega T}\right)\left[\left(\frac{\omega_r}{\omega}\right)^2 + \left(\frac{1}{\omega T}\right)^2 + 1\right]}{\left[\left(\frac{\omega_r}{\omega}\right)^2 - \left(\frac{1}{\omega T}\right)^2 - 1\right]^2 + 4\left(\frac{\omega_r}{\omega}\right)^2\left(\frac{1}{\omega T}\right)^2} \quad . \tag{A-39}$$

The same operation on Equation A-30 for χ' results in

$$\frac{\omega}{\omega_M}\chi' = \frac{\left(\frac{\omega_r}{\omega}\right)\left[\left(\frac{\omega_r}{\omega}\right)^2 + \left(\frac{1}{\omega T}\right)^2 - 1\right]}{\left[\left(\frac{\omega_r}{\omega}\right)^2 - \left(\frac{1}{\omega T}\right)^2 - 1\right]^2 + 4\left(\frac{\omega_r}{\omega}\right)^2\left(\frac{1}{\omega T}\right)^2} \quad . \tag{A-40}$$

Curves of Equations A-39 and A-40 are given in Figures A-1 and A-2 for various values of $\frac{\omega_r}{\omega}$ and ωT. Knowledge of the material characteristics ($4\pi M_s$, H_a, ΔH) would allow one either to fix frequency (and hence ωT) and determine χ' and χ'' as functions of applied field H_o, or to fix the applied field (and hence ω_r) and determine χ' and χ'' as functions of ω. From these generalized curves one can also determine the material characteristics required to achieve desired magnitudes and increments of χ' and χ'' over a specified range of applied field for a given frequency.

As an example of a specific calculation consider a uniaxial anisotropic material for which $\Delta H = 2000$ oersteds, $4\pi M_s = 3500$ gauss, $g = 1.92$ and $H_a = 5000$ oersteds. Let the operating frequency be 9.375 Gc, and therefore $\omega = 58.9 \cdot 10^9$ rad/sec. The familiar curves of μ'' and μ' versus applied field H_o are given for this material in Figure A-3. Fictitious negative values of H_o have been allowed in order to see the resonance shape. For the given material characteristics:

$$\omega_M = \gamma 4\pi M_s = 59.2 \cdot 10^9 \text{ rad/sec}$$

$$\frac{1}{T} = \frac{\gamma \Delta H}{2} = 16.9 \cdot 10^9 \text{ rad/sec}$$

$$\therefore \omega T = 3.485$$

$$\frac{\omega}{\omega_M} = .9956 \approx 1.0.$$

Consider as two particular cases, $H_o = 0$ and $H_o = 1000$ oersteds. This results in:

	$H_o = 0$	$H_o = 1000$
ω_r	$11.407 \cdot 10^{10}$ rad/sec	$13.097 \cdot 10^{10}$ rad/sec
$\frac{\omega_r}{\omega}$	1.937	2.224 ,

and from the generalized curves,

$\mu'' = \chi''$	0.165	0.104
$\mu' = H\chi'$	1.66	1.54

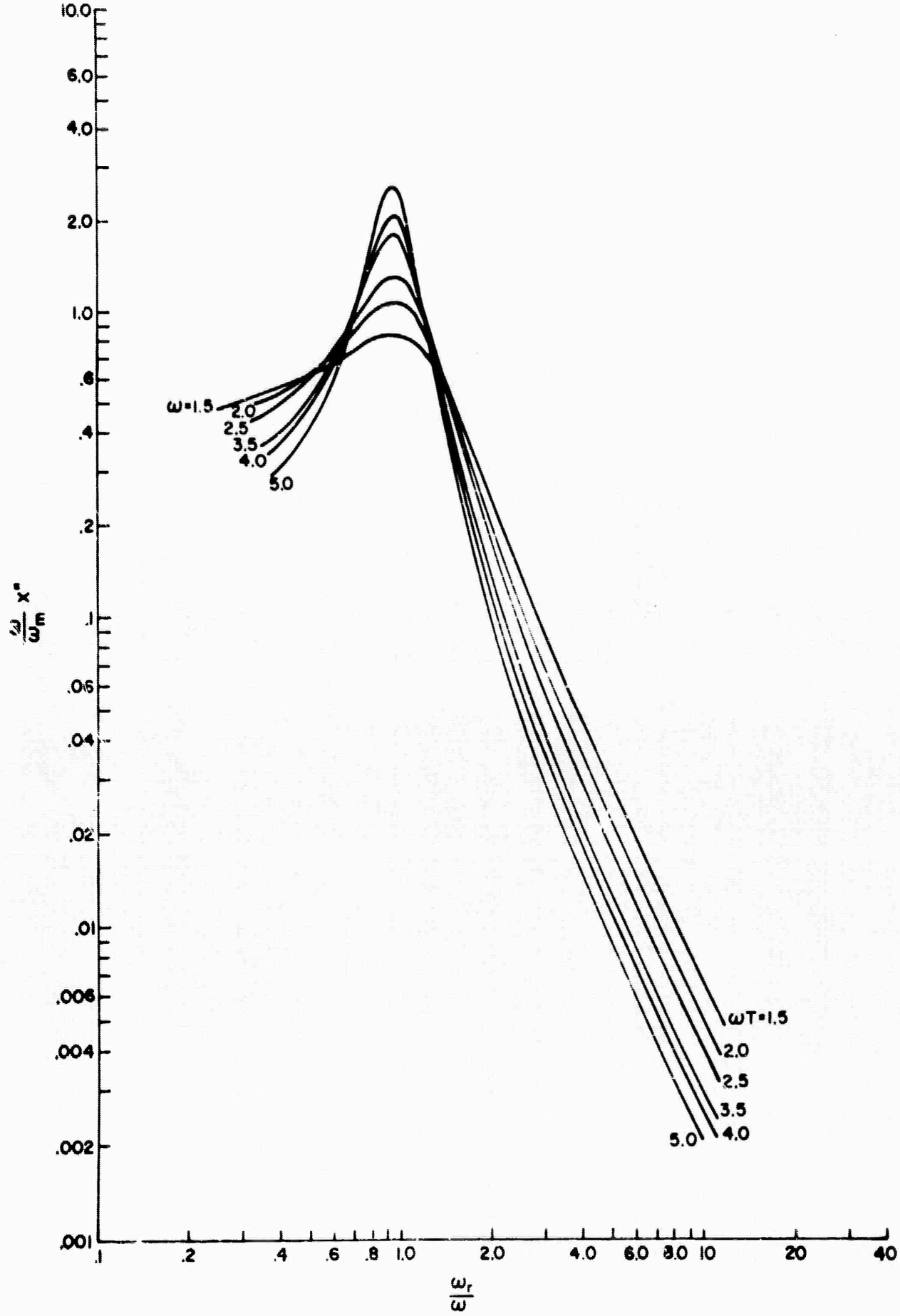

Figure A-1 - Generalized Curves of χ'' as a Function of $\frac{\omega_r}{\omega}$ and $\omega\Gamma$

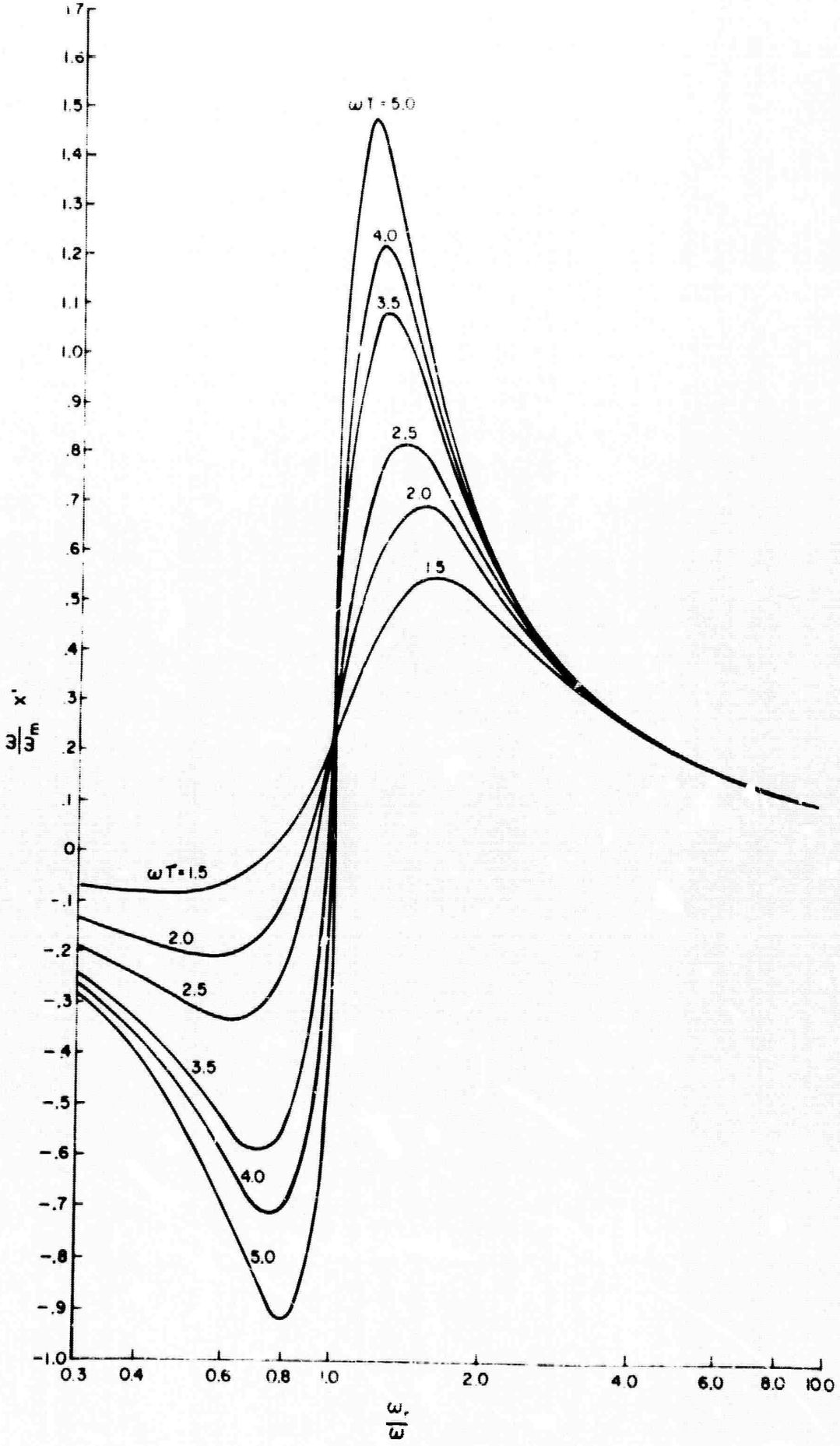

Figure A-2 - Generalized Curves of χ' as a Function of $\frac{\omega_r}{\omega}$ and ωT

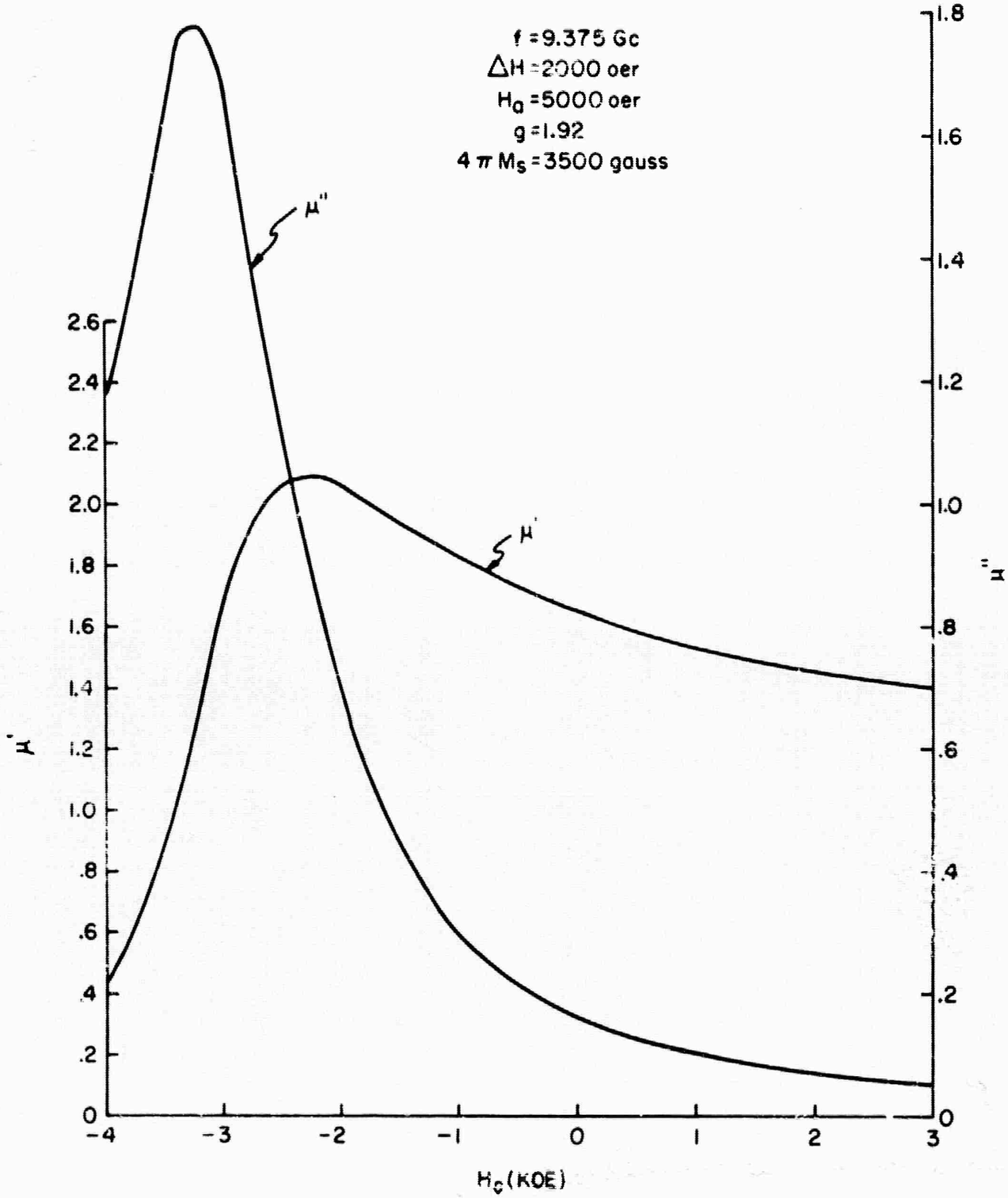

FIG. A-3 – μ' AND μ'' vs APPLIED FIELD, H_a = 5.0 KOE AND ΔH = 2000oer

REFERENCES - APPENDIX A

1. Benjamin Lax and Kenneth J. Button, Microwave Ferrites and Ferrimagnetics, McGraw-Hill Book Company, Inc., New York; 1962.

2. Charles P. Slichter, Principles of Magnetic Resonance, Harper and Row, New York; 1963.

DISTRIBUTION LIST

	No. of Copies
ARPA The Pentagon Washington, D.C. 20301	4
RTD(RTTG) Bolling AFB, D.C. 20332	1
Battelle Memorial Institute Attn: Security Officer 505 King Avenue Columbus 1, Ohio	2
DDC (TISIA-2) Cameron Stn. Alexandria, Virginia	20
RADC (EMATE/Mr. P.A. Romanelli) Griffiss AFB, N.Y. 13442	4
Advisory Group on Electron Devices 356 Broadway New York, Nev York 10013 Attn: Mr. W. Kramer	
Westinghouse Electric Corporation Attn: Mr. G.S. Belvins Electronic Division P.O. Box 1897 Baltimore 3, Maryland	1
The Bendix Corporation Bendix Radio Division Attn: Mr. G. Engelbert Department No. 481 Towson 4, Maryland	1
Hughes Aircraft Company Attn: Mr. Robert A. Moore Building 600 P.O. Box 3310 Fullerton, California 92634	1
General Electric Company Attn: Mr. Hugh Hair Electronics Laboratory Building No. 3 Electronics Park Syracuse, New York	1

DISTRIBUTION LIST (Continued)

	No. of Copies
Sperry Microwave Electronics Company Attn: Mr. B. Duncan Clearwater, Florida	1
Western Microwave Laboratory, Inc. Attn: Mr. T. Giesler 1045 DiGiulie Avenue Santa Clara, California	1

AD _____ ACCESSION NO. _____

Advanced Technology Corp., 1830 York Rd., Timonium, Maryland

HIGH POWER FERRITE PHASE SHIFTER, Semiannual Technical Report, January 1965, Contract No. AF 30(602)-3495, Unclassified Report

6/ pp 3/ illus — tables

Theoretical and experimental investigations of the microwave properties of ferrites at magnetic fields above ferromagnetic resonance are described. The program goal is the development of high power reciprocal phase shifters for X-band and C-band operation. The principal experimental objective is to demonstrate that ferromagnetic losses do not increase with the application of high RF power as typically observed for operations at magnetic fields below resonance. Insertion losses are given as a function of magnetic field strength for samples of nickel-zinc ferrite, manganese-magnesium ferrite and yttrium-iron garnet in a longitudinally magnetized rod configuration. A second absorption peak on the high side of resonance was observed and is identified as a body resonance. The data demonstrates that, at a fixed frequency, the second peak moves toward the ferromagnetic resonance peak as the cross sectional dimensions are reduced.

UNCLASSIFIED

1. Phase Shifters - Development
2. Ferrites - Electromagnetic properties

I. Advanced Technology Corp. Timonium, Md.
II. Rome Air Development Center, Air Force Systems Command, USAF, Griffiss AFB, New York
III. Contract No. AF 30(602)-3495

UNCLASSIFIED

AD _____ ACCESSION NO. _____

Advanced Technology Corp., 1830 York Road, Timonium, Maryland

HIGH POWER FERRITE PHASE SHIFTER, Semiannual Technical Report, January 1965, Contract No. AF 30(602)-3495 Unclassified Report

6/ pp 3/ illus — tables

Theoretical and experimental investigations of the microwave properties of ferrites at magnetic fields above ferromagnetic resonance are described. The program goal is the development of high power reciprocal phase shifters for X-band and C-band operation. The principal experimental objective is to demonstrate that ferromagnetic losses do not increase with the application of high RF power as typically observed for operations at magnetic fields below resonance. Insertion losses are given as a function of magnetic field strength for samples of nickel-zinc ferrite, manganese-magnesium ferrite and yttrium-iron garnet in a longitudinally magnetized rod configuration. A second absorption peak on the high side of resonance was observed and is identified as a body resonance. The data demonstrates that, at a fixed frequency, the second peak moves toward the ferromagnetic resonance peak as the cross sectional dimensions are reduced.

UNCLASSIFIED

1. Phase Shifters - Developmental
2. Ferrites - electromagnetic properties

I. Advanced Technology Corp., Timonium, Md.
II. Rome Air Development Center, Air Force Systems Command, USAF, Griffiss AFB, New York
III. Contract No. AF 30(602)-3495

UNCLASSIFIED

AD _____ ACCESSION NO. _____

Advanced Technology Corp. 1830 York Rd. Timonium, Maryland

HIGH POWER FERRITE PHASE SHIFTER, Semiannual Technical Report, January 1965, Contract No. AF 30(602)-3495 Unclassified Report

6/ pp 3/ illus — tables

Theoretical and experimental investigations of the microwave properties of ferrites at magnetic fields above ferromagnetic resonance are described. The program goal is the development of high power reciprocal phase shifters for X-band and C-band operation. The principal experimental objective is to demonstrate that ferromagnetic losses do not increase with the application of high RF power as typically observed for operations at magnetic fields below resonance. Insertion losses are given as a function of magnetic field strength for samples of nickel-zinc ferrite, manganese-magnesium ferrite and yttrium-iron garnet in a longitudinally magnetized rod configuration. A second absorption peak on the high side of resonance was observed and is identified as a body resonance. The data demonstrates that, at a fixed frequency, the second peak moves toward the ferromagnetic resonance peak as the cross sectional dimensions are reduced.

UNCLASSIFIED

1. Phase Shifters-Development
2. Ferrites - Electromagnetic properties

I. Advanced Technology Corp, Timonium, Md.
II. Rome Air Development Center, Air Force Systems Command, USAF, Griffiss AFB, New York
III. Contract No. AF 30(602)-3495

UNCLASSIFIED

AD _____ ACCESSION NO. _____

Advanced Technology Corp. 1830 York Road, Timonium, Maryland

HIGH POWER FERRITE PHASE SHIFTERS, Semiannual Technical Report, January 1965, Contract No. AF 30(602)-3495 Unclassified Report

6/ pp 3/ illus — tables

Theoretical and experimental investigations of the microwave properties of ferrites at magnetic fields above ferromagnetic resonance are described. The program goal is the development of high power reciprocal phase shifters for X-band and C-band operation. The principal experimental objective is to demonstrate that ferromagnetic losses do not increase with the application of high RF power as typically observed for operations at magnetic fields below resonance. Insertion losses are given as a function of magnetic field strength for samples of nickel-zinc ferrite, manganese-magnesium ferrite and yttrium-iron garnet in a longitudinally magnetized rod configuration. A second absorption peak on the high side of resonance was observed and is identified as a body resonance. The data demonstrates that, at a fixed frequency, the second peak moves toward the ferromagnetic resonance peak as the cross sectional dimensions are reduced.

UNCLASSIFIED

1. Phase Shifter - Developmental
2. Ferrites - electromagnetic properties

I. Advanced Technology Corp., Timonium, Md.
II. Rome Air Development Center, Air Force Systems Command, USAF, Griffiss AFB, New York
III. Contract No. AF 30(602)-3495

UNCLASSIFIED

Insertion loss and phase shift characteristics for oriented uniaxial ferrites are given. The material investigated was $Ni_{.8}Zn_{.2}Co_{.02}W$, a ferrite having a hexagonal crystal structure. It was established that uniaxial ferrites would not be suitable for the subject application because of poor figures of merit. Theoretical computations showed that the governing material characteristic that leads to a poor figure of merit is a large linewidth. The W-type, polycrystalline ferrite typically has a linewidth of 2000 oersteds, which is an order of magnitude larger than that of nickel-zinc ferrite (a cubic crystal structure).
A derivation of the complex susceptibility for ferromagnetic materials and a set of generalized curves for rod geometries with longitudinal magnetic fields are given in the Appendix.

Insertion loss and phase shift characteristics for oriented uniaxial ferrites are given. The material investigated was $Ni_{.8}Zn_{.2}Co_{.02}W$, a ferrite having a hexagonal crystal structure. It was established that uniaxial ferrites would not be suitable for the subject application because of poor figures of merit. Theoretical computations showed that the governing material characteristic that leads to a poor figure of merit is a large linewidth. The W-type, polycrystalline ferrite typically has a linewidth of 2000 oersteds, which is an order of magnitude larger than that of nickel-zinc ferrite (a cubic crystal structure).
A derivation of the complex susceptibility for ferromagnetic materials and a set of generalized curves for rod geometries with longitudinal magnetic fields are given in the Appendix.

Insertion loss and phase shift characteristics for oriented uniaxial ferrites are given. The material investigated was $Ni_{.8}Zn_{.2}Co_{.02}W$, a ferrite having a hexagonal crystal structure. It was established that uniaxial ferrites would not be suitable for the subject application because of poor figures of merit. Theoretical computations showed that the governing material characteristic that leads to a poor figure of merit is a large linewidth. The W-type, polycrystalline ferrite typically has a linewidth of 2000 oersteds, which is an order of magnitude larger than that of nickel-zinc ferrite (a cubic crystal structure).
A derivation of the complex susceptibility for ferromagnetic materials and a set of generalized curves for rod geometries with longitudinal magnetic fields are given in the Appendix.

Insertion loss and phase shift characteristics for oriented uniaxial ferrites are given. The material investigated was $Ni_{.8}Zn_{.2}Co_{.02}W$, a ferrite having a hexagonal crystal structure. It was established that uniaxial ferrites would not be suitable for the subject application because of poor figures of merit. Theoretical computations showed that the governing material characteristic that leads to a poor figure of merit is a large linewidth. The W-type, polycrystalline ferrite typically has a linewidth of 2000 oersteds, which is an order of magnitude larger than that of nickel-zinc ferrite (a cubic crystal structure).
A derivation of the complex susceptibility for ferromagnetic materials and a set of generalized curves for rod geometries with longitudinal magnetic fields are given in the Appendix.